organoids

MDPI

Review

Organoid Models of SARS-CoV-2 Infection: What Have We Learned about COVID-19?

Bang M. Tran [1], Georgia Deliyannis [2], Abderrahman Hachani [2], Linda Earnest [2], Joseph Torresi [2,*] and Elizabeth Vincan [1,3,4,*]

1 Department of Infectious Diseases, Faculty of Medicine, Dentistry and Health Sciences, The Peter Doherty Institute for Infection and Immunity, Melbourne Medical School, The University of Melbourne, Melbourne, VIC 3000, Australia; manht@unimelb.edu.au

2 Department of Microbiology and Immunology, Faculty of Medicine, Dentistry and Health Sciences, The Peter Doherty Institute for Infection and Immunity, School of Biomedical Sciences, The University of Melbourne, Melbourne, VIC 3000, Australia; georgia.deliyannis@unimelb.edu.au (G.D.); abderrahman.hachani@unimelb.edu.au (A.H.); linda.earnest@unimelb.edu.au (L.E.)

3 Victorian Infectious Diseases Reference Laboratory, The Peter Doherty Institute for Infection and Immunity, Melbourne, VIC 3000, Australia

4 Curtin Medical School, Curtin University, Perth, WA 6102, Australia

* Correspondence: josepht@unimelb.edu.au (J.T.); evincan@unimelb.edu.au (E.V.)

Abstract: Severe acute respiratory syndrome coronavirus 2 (SARS-CoV-2) causes coronavirus disease 2019 (COVID-19), which was classified as a pandemic in March 2020. As of 22 January 2022, globally more than 347 million cases of COVID-19 have been diagnosed, with 5.6 million deaths, making it the deadliest pandemic since the influenza pandemic in 1918. The clinical presentation of COVID-19-related illness spans from asymptomatic to mild respiratory symptoms akin to influenza infection to acute symptoms, including pneumonia necessitating hospitalisation and admission to intensive care units. COVID-19 starts in the upper respiratory tract and lungs but in severe cases can also involve the heart, blood vessels, brain, liver, kidneys and intestine. The increasing global health and economic burden of COVID-19 necessitates an urgent and global response. Understanding the functional characteristics and cellular tropism of SARS-CoV-2, and the pathogenesis that leads to multi-organ failure and death, has prompted an unprecedented adoption of organoid models. Successful drug discovery and vaccine development rely on pre-clinical models that faithfully recapitulate the viral life cycle and the host cell response to infection. Human stem cell-derived organoids fulfill these criteria. Here we highlight the role of organoids in the study of SARS-CoV-2 infection and modelling of COVID-19 pathogenesis.

Keywords: COVID-19; SARS-CoV-2; organoid; ex vivo models; infectious disease

1. Modelling Human Infectious Disease with Organoids

Organoids are defined as three-dimensional structures grown from stem cells and consist of organ-specific cell types that self-organize to recapitulate key features and functional characteristics of tissues in a dish [1]. Organoids can be initiated from two main types of stem cells: (1) pluripotent embryonic stem (ES) cells or synthetically induced pluripotent stem (iPS) cells and (2) organ-restricted stem cells. Pluripotent stem cell generated organoids were made more accessible by the discovery by Takahashi and Yamanaka that somatic cells could be taken back ("induced") to pluripotency [2]. Organoids generated from organ-restricted stem cells were first described by the Clevers laboratory in 2009 [3] using mouse intestinal epithelium. Using variations of this intestinal epithelium protocol, organoids have since been established from many organs, especially epithelial tissues. A PubMed search on the term "organoid" shows an exponential increase in publications since 2009 (Figure 1a). Earlier use of the term in the period of 1965–1985 was initiated by developmental biologists to describe tissue explants. Organ-restricted stem cell-derived

organoid technology was embraced to understand tissue homeostasis and regeneration and how cancers start in these tissues (reviewed in [1]). Once it was realized that patient tumor-derived organoids could also be established [4], this led to the establishment of tumor biobanks to understand the processes that lead to cancer growth and to guide treatment [5–7].
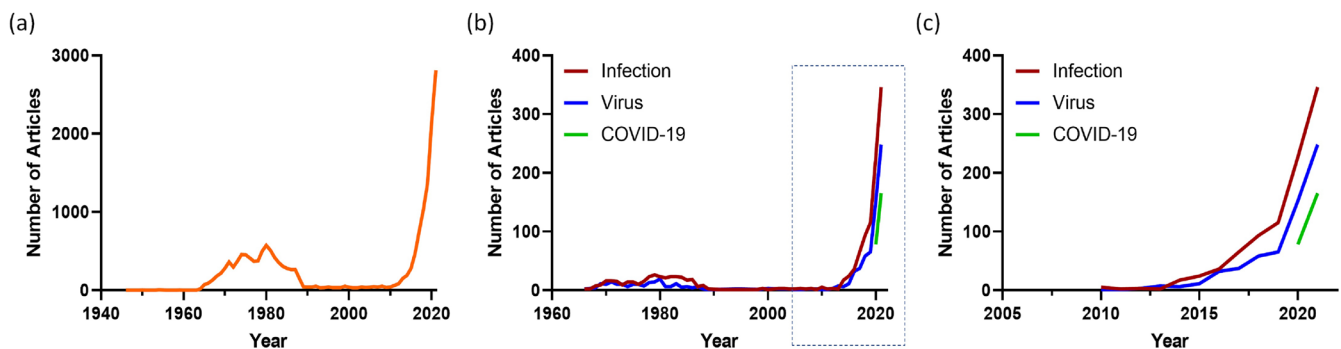

Figure 1. Organoid articles in PubMed. The number of articles published each year for the search term (**a**) "Organoid" and (**b**) "Organoid AND Infection" (red), "Organoid AND Virus" (blue) and "Organoid" AND COVID-19" (green) in PubMed. The boxed section of (**b**) is shown in (**c**).

The infectious disease field was slower on the uptake of organoid technology. Early studies by the Clevers [8] and Estes [9] laboratories demonstrated the utility of tissue stem cell-derived organoids to model respiratory and intestinal infections, respectively, while the Zika virus (ZIKV) outbreak demonstrated the utility of brain organoids established from iPS cells in understanding this disease [10]. However, the adoption of organoids for infectious disease modelling was largely overlooked until the COVID-19 pandemic that has had a devastating impact socially and economically worldwide. This pandemic has triggered the urgent development of medical strategies to tackle COVID-19 and has exposed the limitations of conventional, so called "gold-standard" tissue culture methods used by virologists since the mid 1960's. COVID-19 is a systemic disease and in this review, we highlight the advances made and the insights gained that are attributable to the adoption of organoid technology [11–14]. Half the articles with the PubMed search term "organoids AND infection" for 2021 were COVID-19 studies (Figure 1b,c). The era of organoids modelling infectious disease has arrived [15].

2. Overview of SARS-CoV-2

2.1. Human Coronaviruses

Coronaviruses (CoVs) are enveloped, non-segmented, positive-sense single stranded RNA (ssRNA) viruses that belong to the *Coronaviridea* family and can infect humans and animals [16]. Seven CoVs are known to infect humans, four (human (H)CoV-NL63, HCoV-OC43, HCoV-229E and HCoV-HKU) of which cause mild, seasonal respiratory tract diseases. Three of the seven have emerged over the last 20 years causing severe human disease. Severe acute respiratory syndrome CoV (SARS-CoV), a beta coronavirus, emerged in late 2002 in Guangdong Province, China and spread rapidly from a single index case to five countries and led to large outbreaks, many in tertiary hospitals, with a case fatality of 9.6%. The virus spread to a further seven countries and, in all, resulted in 8098 cases globally with 774 deaths, including many healthcare workers [17]. SARS-CoV is thought to have originated from bats and transmitted from bats to wild animals, such as civets, and then to humans. The epidemic ended in 2004, despite human–human transmission, but possibly resulting from the relatively low infectivity of the virus. In 2012, Middle Eastern Respiratory Syndrome CoV (MERS-CoV) emerged, causing outbreaks of severe pneumonia in Saudi Arabia and South Korea that were associated with a high fatality rate of 34% [18,19]. Imported cases have been reported in several countries, including the United Kingdom, the US, Germany, Italy, Greece, The Netherlands, Malaysia and South Korea. The largest

outbreak occurred in 2014 in Saudi Arabia, with over 500 hospitals involved within a few months. In 2015, a large outbreak across 16 hospitals arising from a single index case occurred in South Korea. The outbreak was finally stopped by quarantining over 17,000 individuals [18]. MERS-CoV is also thought to have originated in bats.

These two highly pathogenic HCoV and the large pool of SARS-CoV-like viruses discovered in bats [20] meant that further zoonotic CoV epidemics and pandemics were highly likely.

2.2. The Emergence of SARS-CoV-2

In December 2019, a novel CoV (initially named "2019-nCoV") emerged in Wuhan, Hubei Province, China, causing severe pneumonia [21]. The virus was found to share 80% homology with SARS-CoV and was subsequently renamed as SARS-CoV-2. Genomic sequencing suggested that the reservoir for SARS-CoV-2 is likely to be bats and pangolins [22–24]. The disease caused by SARS-CoV-2 was soon named coronavirus disease 2019 (COVID-19) and declared a fast-evolving pandemic by the World Health Organization (WHO) on 11 March 2020. This triggered an unprecedented global effort to investigate the characteristics of the virus to develop strategies to diagnose, prevent and treat COVID-19. As of 22 January 2022, more than 347 million cases of COVID-19 have been diagnosed worldwide, with 5.6 million deaths, making it the deadliest pandemic since the influenza pandemic of 1918.

2.3. SARS-CoV-2 Cell Entry

SARS-CoV-2 particles comprise four main structural proteins: spike (S), envelope (E), membrane (M) and nucleocapsid (N) (Figure 2). CoV S proteins are composed of two domains, the receptor binding (S1) and fusion (S2) domains. Viral entry is initiated by the docking of the S protein [25,26] via its receptor binding domain (RBD) in S1 to its cellular receptor. Like SARS-CoV, SARS-CoV-2 uses angiotensin-converting enzyme 2 (ACE2) as its cellular receptor [27,28]. In the respiratory tract, the ACE2 receptor is preferentially expressed on the apical surface of epithelial cells. Both SARS-CoV and SARS-CoV-2 infect by binding apically distributed ACE2 and during their egress from infected cells, are also released from the apical surface of respiratory cells [29–32]. This is significant as our understanding of viral entry, release and neutralization may be guided very differently by studying these events in polarized, compared to non-polarized, respiratory epithelial cells.

Notably, the S protein of SARS-CoV-2 shares only ~73% homology with the S protein of SARS-CoV. The SARS-CoV-2 S protein has an insertion of four amino acids at the S1/S2 junction, known as the multibasic cleavage site (MBCS), rendering it more efficiently cleaved by cellular proteases [27,33]. Cleavage of the spike protein by the cellular serine protease, transmembrane protease serine 2 (TMPRSS2), is required to transform the SARS-CoV-2 spike protein into a fusogenic state, which initiates direct fusion between viral and cellular membranes [34] (Figure 2). The SARS-CoV-2 infection of primary cells is dependent on TMPRSS2 cleavage [33,34]. In continuous cell lines, such as Vero cells established from African Green Monkey kidney epithelium [35], the SARS-CoV-2 uses the endocytic entry pathway wherein the gradual endosomal acidification activates cathepsins that effectively prime the S protein to initiate entry [33,36]. Notably, SARS-CoV-2 binds to human ACE2 more strongly than SARS-CoV [27,28] due to several residue substitutions in its RBD that stabilize the binding domains [37]. Mutations to SARS-CoV-2 spike protein, especially in the RBD, have arisen during the COVID-19 pandemic with emerging variants outcompeting pre-existing circulating isolates. This poses a challenge to vaccine development and antiviral discovery.
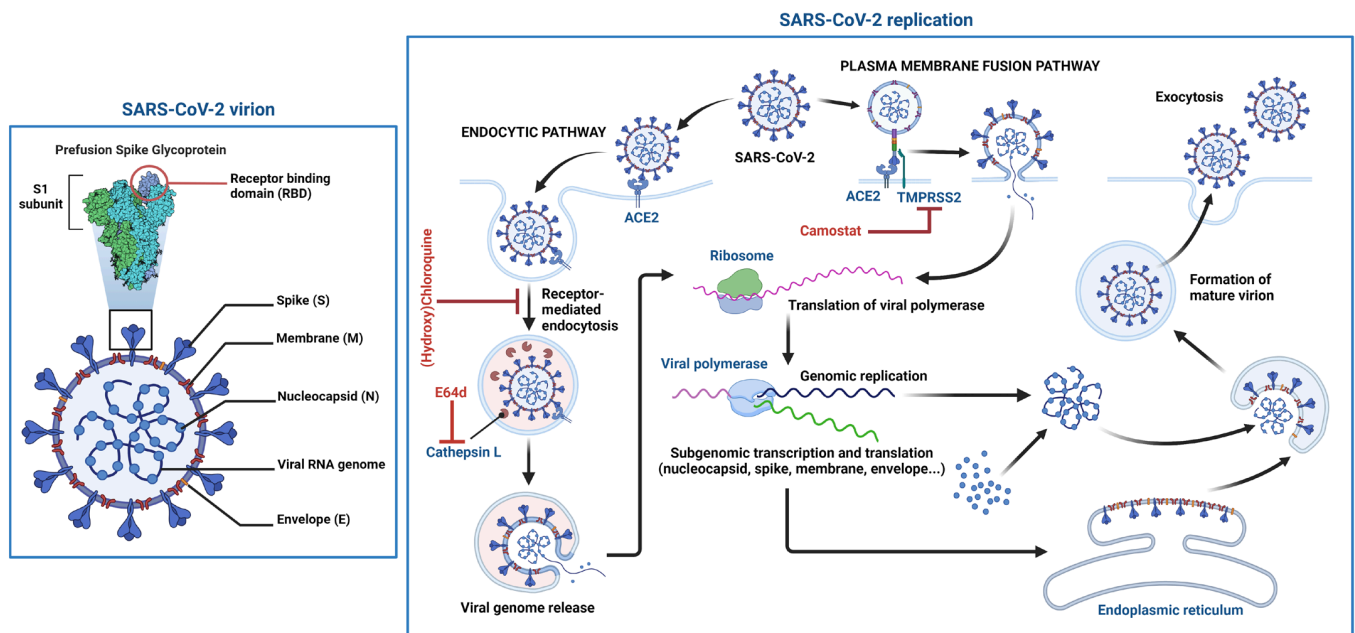
Figure 2. Schematic structure of the SARS-CoV-2 virion and the viral life cycle. The SARS-CoV-2 virion contains an envelope with three proteins: the spike (S) protein, membrane (M) and envelope (E) proteins. The viral RNA genome and the nucleocapsid (N) protein are contained inside the particle. The virion schematic shows in more detail the S protein subunit 1 (S1) containing the receptor binding domain (RBD). The SARS-CoV-2 replication cycle shows two modes of viral entry (endocytic and TMPRSS2-mediated pathways). Both require docking to ACE2 at the cell surface and release of the viral genome into the cytoplasm via membrane fusion. The endocytic pathway is inhibited by (hydroxy)chloroquine and E64d, while TMPRSS2-mediated entry is inhibited by camostat. After synthesis of viral genome and proteins, viral particles are assembled and exit the infected cell. Figure 2 was created with BioRender.com.

2.4. Emergence of SARS-CoV-2 Mutants

Since the emergence and persistence of SARS-CoV-2 in the global population, the virus has undergone several mutational shifts towards variants carrying combinations of changes within the S1 domain of the S protein, in addition to those already occurring in the RBD, enhancing their affinity and binding to the human ACE2 receptor. These mutations resulted in greater virulence and transmissibility and are potentially able to evade neutralizing antibodies (NAb) targeting the RBD and receptor binding motif (RBM) of the spike protein [38–41]. The most frequent variants have included Alpha (B.1.1.7) [42], Beta (B.1.351) [43], Delta (B.1.617.2) [44] and Epsilon (B.1.427/B.1.429) [45], which have been associated with greater transmission and disease severity and, for B.1.351 and B.1.427/B.1.429, escape from neutralization by vaccine-induced antibodies [45–47]. The most recent variant to emerge is Omicron (B.1.529) [48,49]. Being substantially more infectious than Delta, Omicron is not effectively inhibited by vaccine-induced neutralizing antibodies and, in individuals who have received only two doses of COVID-19 vaccines, is associated with reduced vaccine efficacy [50–53].

3. COVID-19 Is a Systemic Disease

SARS-CoV-2 is mainly transmitted through aerosolised respiratory droplets [54]. However, transmission by direct contact and through mucosal membranes is also possible, although they are less likely to transmit infection than close contact with an infected person [55,56]. The basic reproductive number (R0) of the ancestral Wuhan virus and early variants ranged from 2 to 4 [57,58]. For the Delta variant, the R0 is 97% higher than previous variants, making this virus substantially more transmissible [59]. However, with an R0 that

is 4-fold higher than Delta, Omicron became the most transmissible SARS-CoV-2 variant to date [60].

The median incubation period for people who become symptomatic after contact with an infected person is 5 to 6 days for the Wuhan strain [61,62]. In contrast, the incubation period for Delta is 4 days and is shortened to 3 days for Omicron [63]. Both pre-symptomatic and asymptomatic transmissions have been reported [64,65]. Pre-symptomatic transmission occurs 1 to 3 days before symptom onset [66]. The viral load in the upper respiratory tract is highest in the first 3 to 5 days of infection [67], and although the loads are higher in symptomatic individuals, both pre-symptomatic and symptomatic persons can shed high viral loads, readily transmit infection and be associated with high secondary attack rates [68]. The viral load and duration of infectious virus shedding are higher for both the Delta and Omicron variants [69,70].

COVID-19 is a multisystem disease (Figure 3) that starts in the upper respiratory tract and lungs but can also involve the heart, blood vessels, brain, liver, kidneys and intestine [71]. In their majority, patients with COVID-19 present with mild symptoms consisting of fever, cough, loss of taste and/or smell and dyspnea. Other less common symptoms include headache, sore throat, chills, diarrhea, chest pain and myalgias [72]. Whilst most cases resolve without any serious consequences, up to 20% of cases develop moderate to severe disease needing hospitalization. This is more likely to occur in unvaccinated individuals infected with either the Alpha or Delta variants [73,74]. The case fatality rate for infected individuals is approximately 1.9% [75], although this may rise to 8% for people aged 70 to 79 years and to 14.8% for people 80 years and older [76].
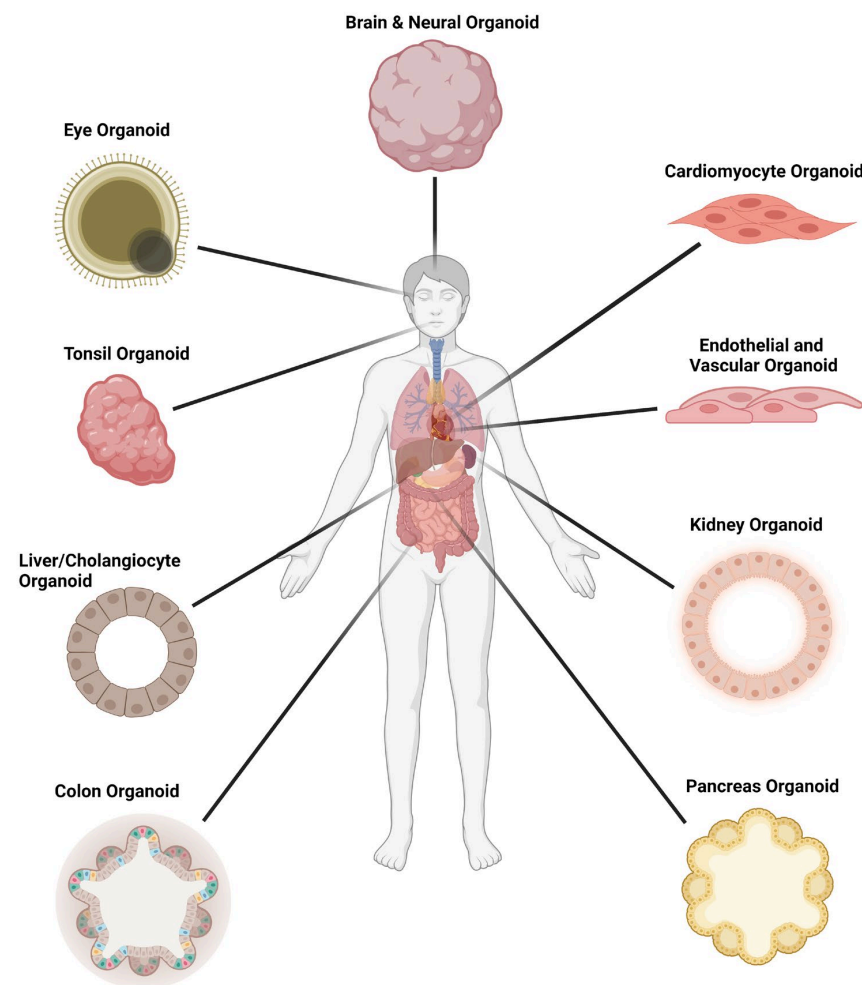

Figure 3. Organoid models used in SARS-CoV-2 infection studies. Figure 3 was created with BioRender.com.

4. Organoid Models of SARS-CoV-2

In vitro models for SARS-CoV-2 infection are essential for the understanding of host and viral factors supporting the cell tropism and the viral replication cycle. They are also needed for preparing viral inoculum for further research and pre-clinical evaluations of medical countermeasures against COVID-19. Early during the pandemic, virologists used classical cell lines such as the immortalized Vero cells and human continuous cell lines. The serious limitations of these simple tissue culture models are that they are not human or are derived from human cancers, and thus do not faithfully replicate healthy human physiology. The Vero cell line has been extensively used by virologists, as these cells have a homozygous gene deletion that causes the loss of the type I interferon (IFN-1) gene cluster and cyclin-dependent kinase inhibitor genes [77,78]. These cells are permissive to diverse viruses, yielding high titers of viral particles in the culture supernatant. However, the SARS-CoV-2 infection of Vero cells leads to the adaptation of the viral genome optimizing their replication in these cells. The MBCS is mutated or deleted in Vero cells [79]. The MBCS facilitates TMPRSS2- mediated entry, and given that this is the mode of entry into primary human epithelial cells [33,80,81], Vero cell-generated viral stocks that do not reflect authentic virus amplification/replication cycles may not recapitulate authentic infection.

The caveat to human cancer cell lines is that they are transformed with multiple changes to the cells' DNA and are also adapted to tissue culture [82]. Yet again, cancer cell lines are far removed from the original cancer and even more so from healthy human tissue. Interestingly, Calu-3 cells, established from a human lung adenocarcinoma, preserve the MBCS and better mimic the SARS-CoV-2 infection of primary epithelial cells than Vero cells [83]. Thus, Calu-3 might provide an intermediary culture system for SARS-CoV-2 propagation. Nonetheless, organoids can reproduce the pathology of COVID-19 of their specific tissue of origin and have been rapidly adopted during COVID-19 (Figure 3). Here, we highlight the diverse human organoids employed in SARS-CoV-2 research.

4.1. Respiratory Tract

COVID-19 was first recognized as causing severe pneumonia; thus, it was vital to identify the regions and cell types of the respiratory tract that are infected with SARS-CoV-2. The respiratory tract architecture changes from a pseudostratified barrier epithelium lining the nose to the delicate monolayer of alveoli, which are small air sacs at the extremities of the lung enabling the exchange of oxygen and carbon dioxide (CO_2) molecules into and out of the bloodstream (Figure 4). The first publications testing the respiratory cell tropism of SARS-CoV-2 used human airway epithelium (HAE) established from progenitor cells (basal cells) isolated from conductive airway tissues resected during surgery. Pseudostratified 3D tissues were differentiated at an air-liquid-interface (ALI) [84,85] or embedded in a matrix [85] (Figure 4). For ALI differentiation, the basal cells are seeded onto transwell membranes, and once confluent across the surface of the membrane, the apical medium is removed, exposing the cells to air. ALI-differentiation medium is refreshed in the basal chamber over 3–4 weeks to generate the pseudostratified tissue. Matrix embedded organoids are similarly seeded in an expansion phase to form cysts, and then changed to an organoid differentiation medium for 3–4 weeks [8,32]. HAE organoids are comprised of several cell types, including basal cells, ciliated cells with apical beating cilia and goblet cells secreting mucous onto the apical surface. These studies confirmed the SARS-CoV-2 infection of ciliated cells, and that viral entry and release occur from the apical surface and was soon confirmed by others [21,84,85]. Using a reporter virus system, RNA in situ hybridization and cultures established from different regions of the respiratory tract, Hou and colleagues [86] demonstrated that the ALI-differentiated nose epithelium expressed the highest levels of ACE2 and TMPRSS2 and showed the greatest SARS-CoV-2 infectivity, which gradually decreased towards the proximal respiratory tract (Figure 4). Early expression studies either did not detect or detected low levels [87] or did not report [85] ACE2 protein expression in respiratory tissues, despite robust protein expression reported in other human tissues such as the intestine analyzed in parallel [85,87]. More recent studies have

confirmed ACE2 protein expression and SARS-CoV-2 infections in respiratory epithelia, identifying the differentiated ciliated cells as the dominant cell type infected [21,29,32,88,89] (reviewed extensively elsewhere, e.g., [90–92]).
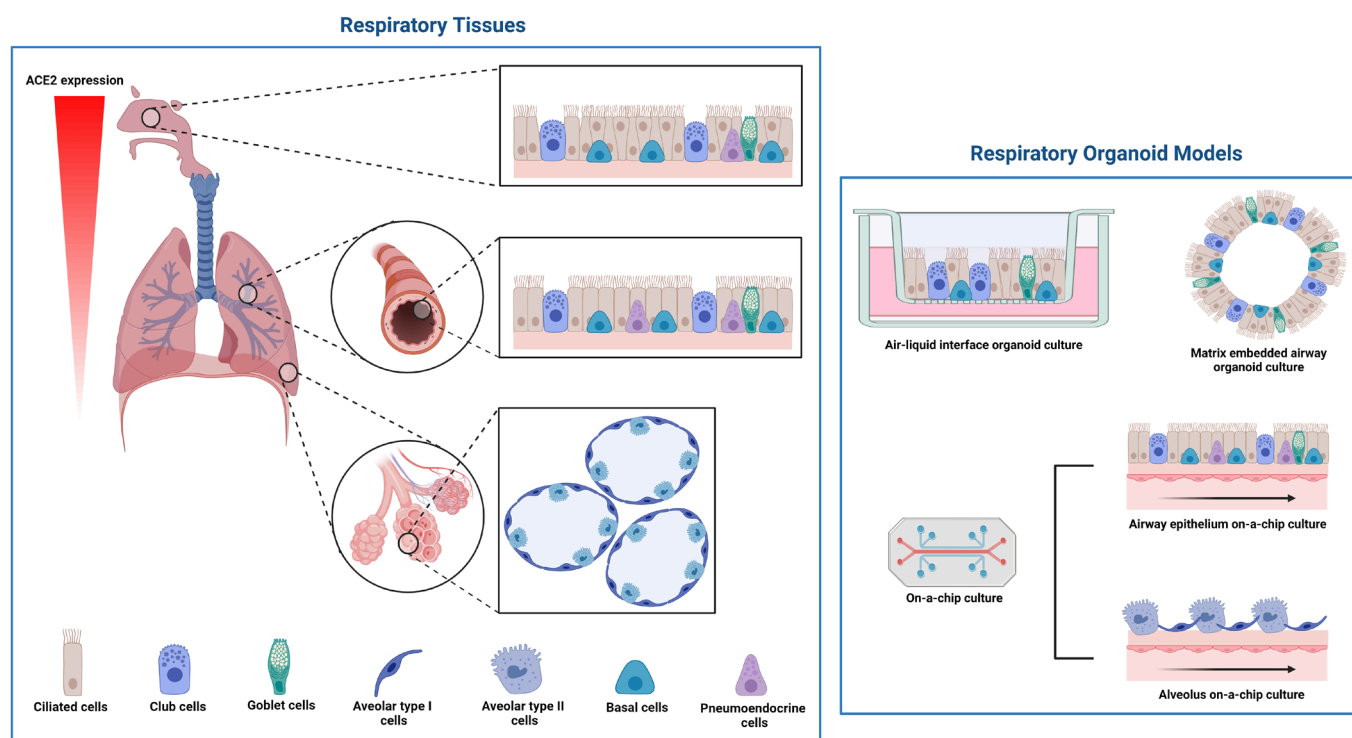

Figure 4. Cell types, and their localization within the respiratory tract, and respiratory organoid models used in SARS-CoV-2 infection studies. The morphology of respiratory tissue changes from the nose epithelium with ciliated, club, goblet, endocrine and basal cells to the delicate structure of alveoli with the flat type I cells and the secretory type II cells. Respiratory organoid culture can be tissue on a membrane (air–liquid–interface), embedded in matrix or microfluidic chip cultures. Figure 4 was created with BioRender.com.

With the urgency to discover and evaluate therapies of severe respiratory damage in COVID-19, researchers have sought to establish human alveolar models of SARS-CoV-2 infection (Figure 4). Unlike primary upper respiratory cells with well-established and characterized ALI culture systems [91], establishing similar cultures of primary alveolar cells proved more difficult. The main cell types of the alveoli sacs are the type I and type II pneumocytes (AT1 and AT2, respectively). Flat AT1 cells mediate gas exchange, while the AT2 cells secrete surfactants. Rare AT2 cells behave as the stem cells of the epithelium and maintain close contact with underlying Wnt-producing fibroblasts. Wnt-producing cells are invariably found in the niche of stem cells. Daughter cells leaving this Wnt-rich niche transdifferentiate into AT1 cells. The AT2 stem cells maintain homeostasis and respond to injury to repair the tissue; they self-renew, recruit AT2 stem cells to the site of injury and generate AT1 cells [93,94]. Recapitulating this level of complexity in tissue culture cannot be mimicked using immortal alveolar cell lines or primary alveolar cells [95]. Recent studies using lung bud tip matrix-embedded organoids to initiate the ALI cultures resulted in patches of bronchiolar and alveolar tissues [96]. SARS-CoV-2 infection demonstrated that in the alveolar regions of the culture, it is the AT2-like cells that support SARS-CoV-2 infection [96]. This has important ramifications for pathogenesis, given that the AT2 cells repair the tissue.

ALI-differentiated cultures established from bronchial lavage or lung resections in a 96-well format have recently been established as a high-throughput research platform (for example, [97]). Several respiratory tissue-derived ALI cultures are now commercially

available (including nose, bronchial and alveolar). Although the cost of the commercial cultures is prohibitive for most research groups, it should accelerate drug discovery and vaccine development undertaken by larger research entities. Respiratory and more complex organoid models on-a-chip (Figure 4) add an additional dimension to the utility of organoid models for studying SARS-CoV-2 infectivity (reviewed elsewhere, for example [98]).

Alternative models for high-throughput platforms have been established using human ES cell-derived lung organoids (hESC-LO) [99]. Here, the ES cells were differentiated into the endoderm, then towards the lung progenitor lineage and finally into differentiated lung cells. RNA-seq on the resultant differentiated lung cells confirmed the presence of AT2 cells expressing ACE2 and TMPRSS2. The alveolar-like organoids were permissive to SARS-CoV-2 infection and upregulated similar cytokine/chemokine genes as observed in lung autopsy tissues of COVID-19 patients [99]. A screen of FDA-approved drugs yielded some targets for follow-up. The main advantage of hES-derived organoids, despite the inability to completely recapitulate human tissue, is that different tissue types can be established from the same ES line, providing a consistent genetic background [1].

4.2. Intestine Epithelium

The first publication using human organoids for SARS-CoV-2 infection was the result of the collaboration between the Clevers and Haagmans laboratories in the Netherlands [85], combining tissue-stem cell derived organoid expertise with virology. The Clevers laboratory identified Leucine-rich, repeat-containing G-protein coupled receptor 5 (Lgr5) as an exclusive maker of adult intestinal epithelial stem cells [100]. They showed that Lgr5$^+$ stem cells generate the different cell types of the epithelium and self-organize into 3D structures that mimic the gut epithelium when embedded in the matrix and provided with stem cell niche growth factors [3,101]. Human small intestinal organoids (hSIOs) can be expanded indefinitely and cryopreserved, providing a renewable resource. The hSIOs can be cultured and embedded into a matrix or grown at ALI [9]. hSIOs [85] and tissues [87] abundantly express ACE2 and support infection by SARS-CoV and SARS-CoV-2 [85]. Methodologies to clone and genetically engineer hSIOs were already established in the Clevers laboratory and employed to reveal essential host factors for coronavirus infection, demonstrating the power of coupling CRISPR/Cas9 gene editing with organoids [33]. Moreover, the hSIOs together with human alveolar and airway ALI organoids revealed differences between the ancestral SARS-CoV-2 and the Alpha (B.1.1.7) variant. The Alpha variant produced a higher replicative fitness, producing high titers of virus later in infection [102].

The very high levels of ACE2 and TMPRSS2 [103] in hSIOs make them a permissive culture system enabling a wide infection dynamic range and a robust platform for the screening of anti-viral inhibitors. Additionally, there is potential for an oral–fecal route of transmission that requires further investigation. SARS-CoV-2 is an enveloped virus (Figure 2) and would not be expected to survive the harsh gastric environment. However, COVID-19 patients develop gastrointestinal symptoms; SARS-CoV-2 infection is reported to alter the intestinal microbiome, and SARS-CoV-2 RNA is detected in fecal samples [104,105].

4.3. Heart

Some COVID-19 patients develop severe cardiovascular complications, which led to investigations to determine if this was the direct result of the SARS-CoV-2 infection of cardiac tissue or a consequence of systemic disease. Examination by digital PCR, Western blot, immunohistochemistry, immunofluorescence, RNAscope and transmission electron microscopy assays of postmortem cardiac heart tissues of SARS-CoV-2 positive patients who showed no signs of cardiac involvement revealed that cardiomyocytes (CM) were indeed infected. Variable patterns of cardiomyocyte injury were observed [106]. This and other studies [107] examining autopsy tissues confirmed the SARS-CoV-2 presence in the heart and CM injury. To examine the human cardiac tropism of SARS-CoV-2, researchers adopted CM cultures derived from human pluripotent ES cells (hESC-CM) or human iPS cells (hiPS-CM).

The differentiation of hESCs is directed towards mesoderm lineage and then differentiation into spontaneously contracting CM, achieving 85–95% purity [108,109]. hESC-CMs express ACE2, while ES cells, mesoderm and cardiac progenitor cells do not [109]. hESC-CMs also express TMPRESS2, cathepsin L and furin [108], mirroring the expression of healthy human heart tissue (left ventricle) [108]. hESC-CMs are susceptible to SARS-CoV-2 infection, which is inhibited by the ACE2 antibody, camostat and E64d, indicating that cell entry requires docking to ACE2 but can proceed via an endocytic pathway (sensitive to E64d) or TMPRSS2-dependent membrane fusion (sensitive to camostat) [108] (Figure 2).

The differentiation of hiPS cells yields three cardiac cell types: endothelial cells, CM and cardiac fibroblast [107]. Of these, only CM expressed ACE2; all cell types expressed cathepsin L and cathepsin B, and none expressed TMPRSS2. Only the CM were infected with SARS-CoV-2, which was inhibited by an ACE2 antibody and E64d, but not by the TMPRSS2 inhibitors camostat and aprotinin [107]. Consequently, hiPS-CM [107,110] do not recapitulate the TMPRSS2 expression pattern of human heart tissue [108]. The SARS-CoV-2 infection of purified hiPS-CM caused cessation of beating after 72 h [111]; however, it remains to be determined if the cardiac arrest seen in COVID-19 patients [71] is the direct effect of the SARS-CoV-2 infection of the CM.

Despite these caveats, pluripotent stem cell-derived cardiomyocytes have been widely adopted as a platform to identify inhibitors of SARS-CoV-2 infection [108,112] and to recapitulate aspects of the CM damage caused by SARS-CoV-2 infection in humans [107,109–111]. The hES cells and reagents to differentiate them into CM are now commercially available. The indication that SARS-CoV-2 entry into CM may depend on TMPRSS2-mediated fusion or on the endocytic pathway (Figure 2) certainly warrants the inclusion of CM models in cell-type platforms used for screening SARS-CoV-2 medical countermeasures [99].

4.4. Liver

Several continuous cell lines were screened and utilized for SARS-CoV-2 infection experiments, including Huh7 cells, a human hepatocellular carcinoma cell line. The susceptibility of this liver cancer cell line to SARS-CoV-2 infection in vitro and the liver comorbidities associated with COVID-19 in patients with severe disease [113] prompted an analysis of existing single-cell (sc) RNAseq databases for cell types within the liver that express ACE2 and TMPRSS2 and could potentially be infected by SARS-CoV-2 (for example, references [114,115]). An analysis across five different liver tissue types (human fetal, healthy, cirrhotic, tumor and adjacent normal) identified a single subpopulation of human liver that co-expressed ACE2 and TMPRSS2, namely the cholangiocyte-biased progenitor pool [115].

Indeed, using human liver organoids, the SARS-CoV-2 infection of cholangiocytes was subsequently confirmed [116]. Human liver organoids established from biliary duct fragments are bipotent progenitor cells that expand as cystic organoid structures and can be differentiated towards a biliary or hepatic cell fate [117,118]. In their expansion phase, the organoid cells express cholangiocyte markers [116,118], ACE2 and TMPRSS2 and support SARS-CoV-2 infection, leading to the formation of large syncytia [116]. Transcriptomic analysis by scRNAseq revealed the decreased expression of genes involved in barrier functions and bile acid transport following SARS-CoV-2 infection. This study in organoids supports the idea that liver damage in COVID-19 patients might be due to cholangiocyte injury induced by SARS-CoV-2 infection [116]. The advantage of human liver ductal organoids resides in their long-term expansion [118], providing a renewable source of primary cells for SARS-CoV-2 infection.

McCarron and colleagues [119] took organoid technology one step further. Nonalcoholic fatty liver disease (NAFLD) and nonalcoholic steatohepatitis (NASH) are becoming recognized as co-morbidities of COVID-19 [120]. The investigators have established and characterized bipotent ductal organoids from patients with NASH because animal models cannot recapitulate this human pathology. Transcriptomic and functional investigations confirmed that NASH patient-derived organoids recapitulate key features of human NASH. Infection with the SARS-CoV-2-VSV pseudovirus that expresses the SARS-CoV-2 S protein

and requires ACE2 and TMPRSS2 for fusion with the cellular membrane was more efficient in NASH organoids than in organoids established from healthy tissues. Interestingly, increased permissiveness to SARS-CoV-2 was not associated with elevated ACE2 or TMPRSS2 expression but an upregulation of ubiquitin D, a known inhibitor of the interferon antiviral response, in the NASH organoids akin to human NASH liver tissue [119]. Establishing organoids from diseased tissues has the potential to reveal the mechanisms of comorbidities in COVID-19.

4.5. Brain

Initial symptoms, such as headache, dizziness and taste and smell impairment were commonly reported for SARS-CoV-2 patients, but in most cases resolved quickly. More serious indications of neurological disorder include seizures, encephalopathy and cerebrovascular disease [121]. MRI-based screens showed structural damage in the brains of recovering COVID-19 patients, indicating potential long-term neurological effects [122]. SARS-CoV-2 RNA was detected in the cerebral spinal fluid (CSF) of COVID-19 patients with neurological symptoms [123] and in autopsy brain samples [124]. To confirm or deny SARS-CoV-2 infection and identify target cell types in the brain, researchers turned to human brain organoids established from hES cells or hiPS cells. Initial results seemed conflicting, detecting SARS-CoV-2 virus in the neurons but not productive infection [125]. This was confirmed in a systematic test of SARS-CoV-2 neurotropism in region-specific brain organoids (cortical, hippocampal, hypothalamic and mid-brain), which also did not show productive SARS-CoV-2 infection [126]. Subsequent studies with brain organoids that contained choroid plexus epithelium were productively infected, but only in the choroid plexus region of the organoid [126,127]. Tropism for choroid plexus epithelium was confirmed using pure choroid plexus organoids [126]. It is proposed that productive SARS-CoV-2 infection leads to the damage of the epithelium and loss of barrier function, allowing viral entry into the central nervous system (CNS).

Another potential portal of entry into the CNS is from the nasal cavity through the olfactory bulb. An elegant study by Meinhardt and colleagues [128] showed that SARS-CoV-2 can enter the CNS by crossing the neural-mucosal interface in olfactory mucosa. The proximity of mucosal, endothelial and nervous tissue, including olfactory and sensory nerve endings, coupled with the robust SARS-CoV-2 infection of the nasal epithelium, might precipitate entry into the CNS via the olfactory tract. This may explain some of the symptoms of COVID-19, including loss of smell and taste.

4.6. Kidney

ACE2 is strongly expressed in kidney tubules [87,129,130]; SARS-CoV-2 can be detected in urine [131] and in autopsy kidney tissue from SARS-CoV-2-infected patients [132,133], and COVID-19 patients show signs of kidney damage [71,134,135]. To determine if the kidney function decline reported for COVID-19 patients could be due to the infection of kidney cells by SARS-CoV-2, hES-derived kidney epithelium organoids were interrogated. The engineered kidney organoids expressed ACE2 and TMPRSS2 and were infected with SARS-CoV-2, producing infectious virus, and the infection was inhibited by soluble ACE2 [136,137]. Remdesivir, an RNA polymerase inhibitor that blocks viral replication, had an additive anti-viral effect when combined with soluble ACE2 in the kidney organoids [138].

An alternative approach, using normal human kidney proximal tubule epithelial cells, was to establish kidney epithelium organoids embedded in a matrix. The organoids expressed ACE2, and a pseudoviral assay was used to confirm that the SARS-CoV-2 S protein enabled pseudoviral entry into the cells [139]. Notably, conditional reprogramming (CR) conditions were used to establish long-term cultures of the primary kidney epithelial cells in 2D before initiating organoid formation and differentiation in 3D. The CR technique has been used to establish long-term cultures from a variety of tissue types without genetic manipulation [140]. An integrated 2D CR and 3D provides a physiologically relevant

platform for drug discovery and safety evaluation to study kidney function and the innate immunity of kidney cells to viral infection.

4.7. The Eye—An Alternative Route of Entry

Although the respiratory system is considered the primary route for SARS-CoV-2 infection, and the nose epithelium the dominant initial site of infection, observations by ophthalmologists early in the pandemic raised the possibility that the eye was also a route of viral entry [141]. People contracted COVID-19 despite wearing a face mask to protect the respiratory route of entry, which led to investigations of the ocular surface as a site of infection by SARS-CoV-2. The ocular surface includes the cornea, sclera and limbus, and an examination of post-mortem samples demonstrated that these tissues express ACE2 and TMPRSS2 [142,143] and were positive for SARS-CoV-2 S protein by immunofluorescence in samples from SARS-CoV-2 positive cadavers [142]. To confirm that these tissue cell types were indeed susceptible to SARS-CoV-2 infection, cultures were established from cells isolated from eye regions of healthy donors and infected with SARS-CoV-2. The limbus cells were the most susceptible primary ocular tissue to SARS-CoV-2 infection [142]. Accessing human eye tissue relies on organ donation, and the cultures established have a limited lifespan and complexity. Human ES cell and iPS cell-derived retinal [144] and "whole eye" [142,145] organoids have been generated and confirm endogenous ACE2 and TMPRSS2 expression [142,146], and that SARS-CoV-2 infection is primarily in limbus-like cells [142,145]. Collectively, these data demonstrate the power of pluripotent stem cell-derived organoid technology in establishing the eye as a potential mode of SARS-CoV-2 transmission and emphasizes the importance of face shields to prevent touching the face or eye, especially in the case of conjunctivitis.

4.8. Vasculature

The vasculature, like neuronal networks, is of great importance to our understanding of COVID-19 pathogenesis as it encompasses all organs. The endothelium lines the inner surface of all blood vessels and plays crucial roles in human physiology and pathophysiology, including COVID-19. The endothelium functions in both adaptive and innate immunity; it provides an anticoagulant surface and maintains blood vessel barrier integrity. The dysregulation of all these functions features in the sequelae of COVID-19 (reviewed extensively, e.g., [147]). However, it remains controversial whether endothelial damage is a direct effect of SARS-CoV-2 infection of the endothelial cells.

Given that severe COVID-19 is a multi-organ disease, the initial focus was on the affected organs. Nonetheless, endothelial damage is causally implicated in COVID-19 organ dysfunction (reviewed extensively, e.g., [147–151]). Early in the pandemic, it was recognized that circulating endothelial cells in COVID-19 patients, which is indicative of endothelial damage, correlated with increases in markers of disease severity and inflammatory cytokines [152,153]. Examinations of autopsy tissues from COVID-19 patients by immunohistochemistry revealed an accumulation of inflammatory cells associated with the endothelium in vascular beds of several organs, including the heart, small intestine and lung [154]. Further examination of kidney post-mortem tissues by electron microscopy showed viral inclusion bodies in the peritubular space and viral particles in endothelial cells of the glomerular capillary loops [154]. The productive SARS-CoV-2 infection of endothelial cells was confirmed using hiPS-derived capillary organoids. Infection of these blood vessel organoids was inhibited by soluble human ACE2, indicating ACE2-mediated viral entry [136]. In a similar vein, Yang and colleagues [155] used hES to generate eight different distinct cell types or organoids modelling the embryonic development of tissues derived from the three germ layers (definitive endoderm, mesoderm and ectoderm). Productive SARS-CoV-2 infection was confirmed in several tissue types, including endothelial cells [155]. Mouse models of SARS-CoV-2 also support the direct infection of lung and cardiac endothelial cells [156].

Nonetheless, the extent to which the direct infection of endothelial cells by SARS-CoV-2 contributes to vascular involvement in COVID-19 remains to be determined and may indeed be organ and tissue dependent. In vitro cultures of primary human umbilical vein endothelial cells (HUVECs) and human microvascular endothelial cells from the lung (HMVEC-L) did not support SARS-CoV-2 infection [157]. These HUVECs and HMVES-L cells expressed very low levels of ACE2 and TMPRSS2 and did not show any morphological changes upon virus exposure to their apical or basal surface. In agreement, Wagner and colleagues [158] could not demonstrate a productive SARS-CoV-2 infection of endothelial cell models established from the vasculature of diverse tissues, irrespective of the SARS-CoV-2 variant used for infection. Virus uptake occurred, but viral replication was not supported. Another study using HUVECs reported that cloned SARS-CoV-2 proteins cause vascular permeability [159]. Resolving these controversies requires further interrogation using physiological human model systems, including more complex organoid models, where the vasculature is embedded within the organoid. For example, hiPS-derived kidney organoids contain multiple renal cell types and structures, as well as the vasculature [160].

Further clear examples of vascular involvement came from COVID-19 infections of children. Although severe COVID-19 illness was rare in children, several cases of acute pediatric vasculitis of unknown origin were diagnosed, initially in Italy and England, and then globally [161–163]. It was described as a Kawasaki-like multisystem inflammatory syndrome [164]. Similar symptoms were later observed in adolescent and adult COVID-19 patients, who did not necessarily present with respiratory manifestations and often tested negative for SARS-CoV-2 by PCR on respiratory swab samples (e.g., [165,166]). The latter implies vasculitis occurs after active infection. Again, direct evidence of productive infection of the endothelium is yet to be determined in these patients.

Further vascular complications in COVID-19 include coagulopathy and resulting thromboembolic events, the exact underlying mechanisms of which are unknown; however, the prophylactic administration of heparin to patients requiring hospitalisation significantly reduced mortality [167,168]. Endothelial dysfunction is also implicated in long COVID-19 by a multicenter observational study of 798 patients [169]. Our understanding of the roles played by the vasculature are far from complete and will undoubtedly fuel the development of more complex organoids.

4.9. Other Organs

Many other organoids derived from tissue stem cells or human pluripotent stem cells have been adopted for SARS-CoV-2 research to define cell tropism and to understand pathogenesis and modes of transmission (Figure 3). These include tonsils and the oral cavity, with saliva as a potential means of transmission, the pancreas, alveolar macrophages and gastric epithelium, to name a few (reviewed comprehensively elsewhere in addition to review articles cited here).

5. Transmission of SARS-CoV-2 from Humans to Animals

Reverse zoonosis is defined as any disease that is spread from humans to animals and tends to occur when there is high prevalence of human infection. With the capacity of coronaviruses to jump species boundaries and adapt to new hosts [170], the reverse zoonosis of SARS-CoV-2 to a wide range of animal species [171] was not unexpected. There are, however, two main concerns with events of reverse zoonosis: firstly, the infected animals may develop severe disease and even die, and secondly, the population of animals in question can become a virus reservoir, from which reintroduction back into humans can take place [172].

During the COVID-19 pandemic, the transmission of SARS-CoV-2 from humans to companion, zoo and farmed animals has been documented [171,173–175] (Figure 5). The first domestic animals to have naturally acquired SARS-CoV-2 infection were cats (*Felis catus*) [176,177], dogs (*Canis lupus familiaris*) [176,178] and pet ferrets (*Mustela putorius furo*) [179,180] living in the same household with COVID-19 patients. The impact of SARS-

CoV-2 infections, through reverse zoonosis on domestic animal health, is unclear as the symptoms reported in these animals ranged from asymptomatic to severe respiratory illness [176]. The airborne transmission of SARS-CoV-2 between cats has also been reported [181].

Among captive wild animals in zoological settings, tigers (*Panthera tigris*) [170,182,183], lions (*Panthera leo*) [170,182], puma (*Puma concolor*) [184], snow leopards (*Panthera uncia*) [185], gorillas (*Gorilla gorilla*) [186,187] and otters (*Aonyx cinereus*) [188] were found to be naturally infected through contact with SARS-CoV-2-infected zoo staff. Animals displayed varying degrees of respiratory illness but recovered. Whether subsequent animal-to-animal transmission occurred is not known.
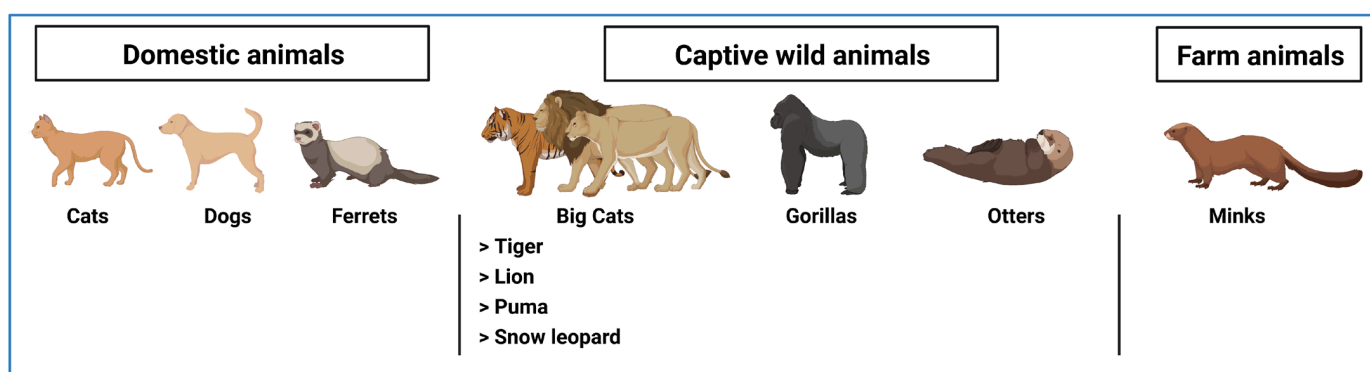

Figure 5. Domestic, captive and farm animal infected with SARS-CoV-2 [170,171,176–194]. Figure 5 was created with BioRender.com.

The human transmission of SARS-CoV-2 to farmed minks has been documented in the United States, Canada and many European countries [171]. Minks exposed to the virus presented mild to severe respiratory distress because of interstitial pneumonia [189]. The origin of the SARS-CoV-2 outbreak could be traced back to the farmers and their close contacts who tested positive for the virus and displayed COVID-19 symptoms [171]. In the United States, the rapid emergence of the N501T (Asn^{501} → Thr) mutation in the RBD of the S protein was observed in farmed minks and detected in 99% of SARS-CoV-2 sequences from minks [190]. Furthermore, Cai et al. [190] demonstrated that the N501T mutation occurred two months earlier in humans than in the minks, suggesting that the variant may have evolved in humans, and was then transmitted to farmed minks with subsequent sustained transmission among the highly susceptible mink population. Minks were suggested as an intermediate host for SARS-CoV-2 adaptation following the identification of a mink-associated variant in Denmark, thus supporting the rapid adaptation of the virus in this animal reservoir [190,191]. These findings were verified by subsequent virus transmissions from infected minks back to humans [192]. The mink mutant proved not to be too dangerous, as there was little evidence that it was more transmissible or more virulent in humans, nor that it could jeopardize the efficacy of therapeutics and vaccines [193]. However, as a precautionary measure, Denmark, the largest producer of mink fur, culled more than 17 million minks to control the spread of COVID-19 in minks and farm workers [193,194].

The analysis of ACE2 protein conservation across species, the modelling of the S viral protein with ACE2 [195–198] and animal infection models [199–211] have highlighted the susceptibility spectrum of many animal species to COVID-19. Some livestock species displayed resistance to experimental infection with SARS-CoV-2 including cattle (*Bos taurus*) [212], and chickens, ducks and pigs [213,214]; however, as it takes only a few mutations or genetic recombination events for the virus to cross species and establish a new host, it is imperative that SARS-CoV-2 occurrence in domestic and farmed animals is monitored. A strategy to help mitigate or contain SARS-CoV-2 transmission could be the

establishment of animal organoid cultures for screening the susceptibility of these animals to new SARS-CoV-2 variants.

6. What Have We Learned from Human Organoid-Based SARS-CoV-2 Research?

6.1. Limitations of Drug Screens on Conventional Cell Lines

Hydroxychloroquine was one of the earliest drugs to be repurposed for COVID-19 treatment. In February 2020, Wang and colleagues were the first to report the effect of chloroquine as an antiviral treatment for SARS-CoV-2 infection [215]. They screened a variety of potential compounds in Vero cells in vitro for inhibition efficacy and cytotoxicity and showed that remdesivir and chloroquine were the best candidates. Shortly later, the same group demonstrated that hydroxychloroquine, a less toxic derivative of chloroquine, was as effective as chloroquine in inhibiting viral replication and infection [216]. While remdesivir performed better, there were many limitations for using remdesivir for COVID-19 treatment on a global scale. Remdesivir was still an experimental drug under patent protection of Gilead, which means the cost for treatment would be prohibitive. The manufacturing process is complicated, and the drug itself must be administered intravenously. Hydroxychloroquine, on the other hand, is widely and cheaply available. It can be taken orally and has been approved for long-term use in humans. These findings with hydroxychloroquine were confirmed by others using Vero and other cell lines, except in Calu-3 [217,218]. However, the urgency for a drug and political pressure led to human trials of hydroxychloroquine before pre-clinical testing was completed. Unsurprisingly, hydroxychloroquine failed clinical trial [219]. We now know that in mouse [220], hamster and nonhuman primate models [221,222] of COVID-19, chloroquine failed to protect against SARS-CoV-2 infection. Much time and money was wasted by this haste.

A detailed study of cellular factors necessary for SARS-CoV-2 entry (Figure 2) using CRISPR/Cas9 gene editing in primary human epithelial organoids verified ACE2 and TMPRSS2 as essential factors for SARS-CoV-2 infection [33]. Infection was inhibited by the TMPRSS2 inhibitor camostat but not hydroxychloroquine, which inhibits receptor-mediated endocytosis. Furthermore, the Alpha variant of SARS-CoV-2 (B.1.1.7), SARS-CoV and MERS similarly depended on TMPRSS2 [33]. Had the early drug screens included primary epithelial cells, hydroxychloroquine would not have been considered a viable candidate for clinical trial at that time.

A further caveat to using Vero cells for antiviral drug screens and viral neutralization assays, which are considered by virologists as the "gold standard", is that, as already mentioned above, viral infection cannot induce an IFN-I response in these cells, and thus any effect of drugs or neutralizing antibodies may not translate to humans. Furthermore, Vero cells are not human- but monkey kidney-derived and may not predict toxicity to human cells.

6.2. Clinical Isolates and Viral Stocks

The authenticity of the cell model is paramount to ensuring the validity of pre-clinical tests, but so is the authenticity of the virus. As we have alluded to already, SARS-CoV, MERS and SARS-CoV-2 enter cells by docking to ACE2 followed by TMPRSS2-mediated cleavage of the S protein to initiate fusion. The fusion can be with the plasma membrane or from an endosome (Figure 2). Unlike SARS-CoV and CoV-MERS, SARS-CoV-2 has MBCS that facilitates TMPRSS2-mediated cleavage and, consequently, speed and efficiency of viral entry [80,223]. This is the preferred mode of entry into primary respiratory cells as these express high levels of TMPRSS2 but low levels of cathepsins [80]. SARS-CoV-2 stocks prepared in Vero cells can harbor mutations in or deletions of the MBCS [79,80,223,224] affecting the ability of the virus to infect human airway cells and viral transmission from infected to uninfected animals [225]. These mutations were rarely observed in clinical samples [226]. Propagation of SARS-CoV-2 in Calu-3 cells and primary airway epithelium preserves the authenticity of the S protein. Although Calu-3 is a cancer cell line and consequently far removed from primary airway epithelial cells, it expresses high levels of

TMPRSS2 [80] and provides an intermediary renewable culture system for propagating viral stocks that, at least for the SARS-CoV-2 variants tested to date, preserves virus authenticity [83].

6.3. Accurate Pre-Clinical Models of SARS-CoV-2 Transmission and Respiratory Disease

ALI-HNE and matrix-embedded HNE organoids are proving to be excellent models of SARS-CoV-2 variant transmissibility [32,227,228]. Infection of ALI-HNE with an ancestral (Wuhan) clinical isolate [229] did not cause overt cytopathic effects, despite yielding a high titer virus from the apical surface. In stark contrast, infection with the Delta (B.1.617.2) variant induced large syncytia and extensive damage to the epithelium [32]. This difference between the viruses was corroborated by fusogenicity assays [228] and was attributed to the P681R mutation in the S protein of Delta [227]. Delta caused similar cytopathic effects in human alveolar organoids and in the lungs of hamsters, causing damage to the alveolar pneumocytes and inducing macrophage infiltration [227]. The fusogenicity and pathogenicity of Delta might underlie the increased transmissibility and rapid spread of Delta globally [230] and the severity of the illness caused.

Early studies with the most recent variant Omicron (B.1.529) in ALI-HNE show more rapid viral kinetics than Delta [231], which may underlie the increased transmissibility and rapid global spread of this variant [48]. However, compared to Delta, syncytia formation is diminished [52,231], as is pathogenicity in mouse and hamster models [232,233] and human lung alveolar organoids [52]. Reduced pathogenicity in human alveolar organoids might indicate decreased severity of disease in the real-world human experience with Omicron. Abdullah and colleagues [234] compared the 466 hospital COVID-19 admissions since 14 November 2021 to the 3962 admissions since 4 May 2020, prior to the Omicron outbreak, in the Omicron-driven fourth wave in the City of Tshwane, Gauteng Province, South Africa, its first global epicenter. COVID-19 disease severity was decreased in the Omicron wave. However, the extent that this decreased severity can be attributed to viral factors, as opposed to immunization status, for example, remains to be determined. Nonetheless, the organoid models were predictive of immune evasion by Omicron [52], the structural basis of which has recently been attributed to specific mutations in the S protein [235].

Collectively, the primary human respiratory organoids established from different regions of the respiratory tract offer insights into viral transmissibility and pathogenicity of SARS-CoV-2 variants as they emerge and the potential for immune evasion.

7. Conclusions and Perspectives

The SARS-CoV-2 pandemic has seen an unprecedented advancement in diverse fields: genomic epidemiology and modelling, vaccine and drug development, pre-clinical models and public health, to name a few. Additionally, it has revealed shortcomings in each of these as measures were introduced to control the pandemic. In the early phase of the pandemic, the focus was on the non-functional characteristics, such as genomics, phylogeny and evolution of SARS-CoV-2. It soon became evident that COVID-19 was more than a respiratory infection, and functional characteristics such as mechanisms of cell entry and cell tropism, host cell response to infection and the development of vaccines and drugs to treat COVID-19 became, and are still, paramount. Advances in our understanding of functional characteristics require authentic pre-clinical models.

The need to understand the underlying drivers of SARS-CoV-2 mutations, the clinical impact of emerging variants and the multi-organ clinical sequelae of severe COVID-19, has led to an exponential adoption of organoids from diverse tissues. Through organoid technology, we gained an understanding of potential viral entry points (nose, eye), a potential loss of epithelial barrier function to gain access to the brain/CNS (choroid plexus, olfactory bulb) and are beginning to understand the role of comorbidities (NASH). Early studies of autopsy tissue identified the organs harboring SARS-CoV-2. Tissue and region-specific

organoids helped identify the target cells within the tissue of affected organs (e.g., lung, liver, kidney, brain and vasculature).

The limitations of classical virology tissue culture models were quickly revealed, which led to the use of more predictive organoid-based cultures in drug discovery and vaccine feasibility studies. The diverse human organoid pre-clinical models provide insight into transmissibility and pathogenesis. The next phase is organoid models with more complexity, incorporating components of the cellular and physical microenvironment of infected cells. Understanding the long-term effects of COVID-19, referred to as "long-COVID", for example, remains a challenge and will undoubtedly fuel further adoption and advancement of organoid models.

References

1. Clevers, H. Modeling Development and Disease with Organoids. *Cell* **2016**, *165*, 1586–1597. [CrossRef] [PubMed]
2. Takahashi, K.; Yamanaka, S. Induction of pluripotent stem cells from mouse embryonic and adult fibroblast cultures by defined factors. *Cell* **2006**, *126*, 663–676. [CrossRef] [PubMed]
3. Sato, T.; Vries, R.G.; Snippert, H.J.; van de Wetering, M.; Barker, N.; Stange, D.E.; van Es, J.H.; Abo, A.; Kujala, P.; Peters, P.J.; et al. Single Lgr5 stem cells build crypt-villus structures in vitro without a mesenchymal niche. *Nature* **2009**, *459*, 262–265. [CrossRef] [PubMed]
4. Van de Wetering, M.; Francies, H.E.; Francis, J.M.; Bounova, G.; Iorio, F.; Pronk, A.; van Houdt, W.; van Gorp, J.; Taylor-Weiner, A.; Kester, L.; et al. Prospective derivation of a living organoid biobank of colorectal cancer patients. *Cell* **2015**, *161*, 933–945. [CrossRef] [PubMed]
5. Tuveson, D.; Clevers, H. Cancer modeling meets human organoid technology. *Science* **2019**, *364*, 952–955. [CrossRef] [PubMed]
6. Vlachogiannis, G.; Hedayat, S.; Vatsiou, A.; Jamin, Y.; Fernandez-Mateos, J.; Khan, K.; Lampis, A.; Eason, K.; Huntingford, I.; Burke, R.; et al. Patient-derived organoids model treatment response of metastatic gastrointestinal cancers. *Science* **2018**, *359*, 920–926. [CrossRef]
7. Sharma, A.; Cao, E.Y.; Kumar, V.; Zhang, X.; Leong, H.S.; Wong, A.M.L.; Ramakrishnan, N.; Hakimullah, M.; Teo, H.M.V.; Chong, F.T.; et al. Longitudinal single-cell RNA sequencing of patient-derived primary cells reveals drug-induced infidelity in stem cell hierarchy. *Nat. Commun.* **2018**, *9*, 4931. [CrossRef]
8. Sachs, N.; Papaspyropoulos, A.; Zomer-van Ommen, D.D.; Heo, I.; Bottinger, L.; Klay, D.; Weeber, F.; Huelsz-Prince, G.; Iakobachvili, N.; Amatngalim, G.D.; et al. Long-term expanding human airway organoids for disease modeling. *EMBO J.* **2019**, *38*, e100300. [CrossRef] [PubMed]
9. Ettayebi, K.; Crawford, S.E.; Murakami, K.; Broughman, J.R.; Karandikar, U.; Tenge, V.R.; Neill, F.H.; Blutt, S.E.; Zeng, X.L.; Qu, L.; et al. Replication of human noroviruses in stem cell-derived human enteroids. *Science* **2016**, *353*, 1387–1393. [CrossRef]
10. Qian, X.; Nguyen, H.N.; Song, M.M.; Hadiono, C.; Ogden, S.C.; Hammack, C.; Yao, B.; Hamersky, G.R.; Jacob, F.; Zhong, C.; et al. Brain-Region-Specific Organoids Using Mini-bioreactors for Modeling ZIKV Exposure. *Cell* **2016**, *165*, 1238–1254. [CrossRef]

11. Synowiec, A.; Szczepanski, A.; Barreto-Duran, E.; Lie, L.K.; Pyrc, K. Severe Acute Respiratory Syndrome Coronavirus 2 (SARS-CoV-2): A Systemic Infection. *Clin. Microbiol. Rev.* **2021**, *34*, e00133-20. [CrossRef] [PubMed]
12. Kim, T.; Lee, J.S.; Ju, Y.S. Experimental Models for SARS-CoV-2 Infection. *Mol. Cells* **2021**, *44*, 377–383. [CrossRef] [PubMed]
13. Geurts, M.H.; van der Vaart, J.; Beumer, J.; Clevers, H. The Organoid Platform: Promises and Challenges as Tools in the Fight against COVID-19. *Stem Cell Rep.* **2021**, *16*, 412–418. [CrossRef]
14. Takayama, K. In Vitro and Animal Models for SARS-CoV-2 research. *Trends Pharmacol. Sci.* **2020**, *41*, 513–517. [CrossRef]
15. Mallapaty, S. The mini lungs and other organoids helping to beat COVID. *Nature* **2021**, *593*, 492–494. [CrossRef]
16. Fung, T.S.; Liu, D.X. Human Coronavirus: Host-Pathogen Interaction. *Annu. Rev. Microbiol.* **2019**, *73*, 529–557. [CrossRef]
17. Hui, D.S.; Chan, M.C.; Wu, A.K.; Ng, P.C. Severe acute respiratory syndrome (SARS): Epidemiology and clinical features. *Postgrad. Med. J.* **2004**, *80*, 373–381. [CrossRef]
18. Fehr, A.R.; Channappanavar, R.; Perlman, S. Middle East Respiratory Syndrome: Emergence of a Pathogenic Human Coronavirus. *Annu. Rev. Med.* **2017**, *68*, 387–399. [CrossRef]
19. Arabi, Y.M.; Balkhy, H.H.; Hayden, F.G.; Bouchama, A.; Luke, T.; Baillie, J.K.; Al-Omari, A.; Hajeer, A.H.; Senga, M.; Denison, M.R.; et al. Middle East Respiratory Syndrome. *N. Engl. J. Med.* **2017**, *376*, 584–594. [CrossRef]
20. Hu, B.; Zeng, L.P.; Yang, X.L.; Ge, X.Y.; Zhang, W.; Li, B.; Xie, J.Z.; Shen, X.R.; Zhang, Y.Z.; Wang, N.; et al. Discovery of a rich gene pool of bat SARS-related coronaviruses provides new insights into the origin of SARS coronavirus. *PLoS Pathog.* **2017**, *13*, e1006698. [CrossRef]
21. Zhu, N.; Zhang, D.; Wang, W.; Li, X.; Yang, B.; Song, J.; Zhao, X.; Huang, B.; Shi, W.; Lu, R.; et al. A Novel Coronavirus from Patients with Pneumonia in China, 2019. *N. Engl. J. Med.* **2020**, *382*, 727–733. [CrossRef] [PubMed]
22. Lu, R.; Zhao, X.; Li, J.; Niu, P.; Yang, B.; Wu, H.; Wang, W.; Song, H.; Huang, B.; Zhu, N.; et al. Genomic characterisation and epidemiology of 2019 novel coronavirus: Implications for virus origins and receptor binding. *Lancet* **2020**, *395*, 565–574. [CrossRef]
23. Zhou, P.; Yang, X.L.; Wang, X.G.; Hu, B.; Zhang, L.; Zhang, W.; Si, H.R.; Zhu, Y.; Li, B.; Huang, C.L.; et al. A pneumonia outbreak associated with a new coronavirus of probable bat origin. *Nature* **2020**, *579*, 270–273. [CrossRef]
24. Wu, F.; Zhao, S.; Yu, B.; Chen, Y.M.; Wang, W.; Song, Z.G.; Hu, Y.; Tao, Z.W.; Tian, J.H.; Pei, Y.Y.; et al. A new coronavirus associated with human respiratory disease in China. *Nature* **2020**, *579*, 265–269. [CrossRef]
25. Ke, Z.; Oton, J.; Qu, K.; Cortese, M.; Zila, V.; McKeane, L.; Nakane, T.; Zivanov, J.; Neufeldt, C.J.; Cerikan, B.; et al. Structures and distributions of SARS-CoV-2 spike proteins on intact virions. *Nature* **2020**, *588*, 498–502. [CrossRef]
26. Turonova, B.; Sikora, M.; Schurmann, C.; Hagen, W.J.H.; Welsch, S.; Blanc, F.E.C.; von Bulow, S.; Gecht, M.; Bagola, K.; Horner, C.; et al. In situ structural analysis of SARS-CoV-2 spike reveals flexibility mediated by three hinges. *Science* **2020**, *370*, 203–208. [CrossRef]
27. Walls, A.C.; Park, Y.J.; Tortorici, M.A.; Wall, A.; McGuire, A.T.; Veesler, D. Structure, Function, and Antigenicity of the SARS-CoV-2 Spike Glycoprotein. *Cell* **2020**, *183*, 1735. [CrossRef]
28. Wrapp, D.; Wang, N.; Corbett, K.S.; Goldsmith, J.A.; Hsieh, C.L.; Abiona, O.; Graham, B.S.; McLellan, J.S. Cryo-EM structure of the 2019-nCoV spike in the prefusion conformation. *Science* **2020**, *367*, 1260–1263. [CrossRef]
29. Jia, H.P.; Look, D.C.; Shi, L.; Hickey, M.; Pewe, L.; Netland, J.; Farzan, M.; Wohlford-Lenane, C.; Perlman, S.; McCray, P.B., Jr. ACE2 receptor expression and severe acute respiratory syndrome coronavirus infection depend on differentiation of human airway epithelia. *J. Virol.* **2005**, *79*, 14614–14621. [CrossRef]
30. Tseng, C.T.; Tseng, J.; Perrone, L.; Worthy, M.; Popov, V.; Peters, C.J. Apical entry and release of severe acute respiratory syndrome-associated coronavirus in polarized Calu-3 lung epithelial cells. *J. Virol.* **2005**, *79*, 9470–9479. [CrossRef]
31. Ren, X.; Glende, J.; Al-Falah, M.; de Vries, V.; Schwegmann-Wessels, C.; Qu, X.; Tan, L.; Tschernig, T.; Deng, H.; Naim, H.Y.; et al. Analysis of ACE2 in polarized epithelial cells: Surface expression and function as receptor for severe acute respiratory syndrome-associated coronavirus. *J. Gen. Virol.* **2006**, *87*, 1691–1695. [CrossRef]
32. Tran, B.M.; Grimley, S.L.; McAuley, J.L.; Hachani, A.; Earnest, L.; Wong, S.L.; Caly, L.; Druce, J.; Purcell, D.F.J.; Jackson, D.C.; et al. Air-Liquid-Interface Differentiated Human Nose Epithelium: A Robust Primary Tissue Culture Model of SARS-CoV-2 Infection. *Int. J. Mol. Sci.* **2022**, *23*, 835. [CrossRef]
33. Beumer, J.; Geurts, M.H.; Lamers, M.M.; Puschhof, J.; Zhang, J.; van der Vaart, J.; Mykytyn, A.Z.; Breugem, T.I.; Riesebosch, S.; Schipper, D.; et al. A CRISPR/Cas9 genetically engineered organoid biobank reveals essential host factors for coronaviruses. *Nat. Commun.* **2021**, *12*, 5498. [CrossRef] [PubMed]
34. Hoffmann, M.; Kleine-Weber, H.; Schroeder, S.; Kruger, N.; Herrler, T.; Erichsen, S.; Schiergens, T.S.; Herrler, G.; Wu, N.H.; Nitsche, A.; et al. SARS-CoV-2 Cell Entry Depends on ACE2 and TMPRSS2 and Is Blocked by a Clinically Proven Protease Inhibitor. *Cell* **2020**, *181*, 271–280. [CrossRef] [PubMed]
35. Yasumura, Y.; Kawakita, M. The research for the SV40 by means of tissue culture technique. *Nippon Rinsho* **1963**, *21*, 1201–1219.
36. Hoffmann, M.; Mosbauer, K.; Hofmann-Winkler, H.; Kaul, A.; Kleine-Weber, H.; Kruger, N.; Gassen, N.C.; Muller, M.A.; Drosten, C.; Pohlmann, S. Chloroquine does not inhibit infection of human lung cells with SARS-CoV-2. *Nature* **2020**, *585*, 588–590. [CrossRef]
37. Shang, J.; Ye, G.; Shi, K.; Wan, Y.; Luo, C.; Aihara, H.; Geng, Q.; Auerbach, A.; Li, F. Structural basis of receptor recognition by SARS-CoV-2. *Nature* **2020**, *581*, 221–224. [CrossRef]

38. Korber, B.; Fischer, W.M.; Gnanakaran, S.; Yoon, H.; Theiler, J.; Abfalterer, W.; Hengartner, N.; Giorgi, E.E.; Bhattacharya, T.; Foley, B.; et al. Tracking Changes in SARS-CoV-2 Spike: Evidence that D614G Increases Infectivity of the COVID-19 Virus. *Cell* **2020**, *182*, 812–827. [CrossRef]

39. Zhang, L.; Jackson, C.B.; Mou, H.; Ojha, A.; Peng, H.; Quinlan, B.D.; Rangarajan, E.S.; Pan, A.; Vanderheiden, A.; Suthar, M.S.; et al. SARS-CoV-2 spike-protein D614G mutation increases virion spike density and infectivity. *Nat. Commun.* **2020**, *11*, 6013. [CrossRef]

40. Weisblum, Y.; Schmidt, F.; Zhang, F.; DaSilva, J.; Poston, D.; Lorenzi, J.C.; Muecksch, F.; Rutkowska, M.; Hoffmann, H.H.; Michailidis, E.; et al. Escape from neutralizing antibodies by SARS-CoV-2 spike protein variants. *eLife* **2020**, *9*, e61312. [CrossRef]

41. Ou, J.; Zhou, Z.; Dai, R.; Zhang, J.; Zhao, S.; Wu, X.; Lan, W.; Ren, Y.; Cui, L.; Lan, Q.; et al. V367F Mutation in SARS-CoV-2 Spike RBD Emerging during the Early Transmission Phase Enhances Viral Infectivity through Increased Human ACE2 Receptor Binding Affinity. *J. Virol.* **2021**, *95*, e0061721. [CrossRef] [PubMed]

42. Davies, N.G.; Abbott, S.; Barnard, R.C.; Jarvis, C.I.; Kucharski, A.J.; Munday, J.D.; Pearson, C.A.B.; Russell, T.W.; Tully, D.C.; Washburne, A.D.; et al. Estimated transmissibility and impact of SARS-CoV-2 lineage B.1.1.7 in England. *Science* **2021**, *372*, eabg3055. [CrossRef] [PubMed]

43. Tegally, H.; Wilkinson, E.; Giovanetti, M.; Iranzadeh, A.; Fonseca, V.; Giandhari, J.; Doolabh, D.; Pillay, S.; San, E.J.; Msomi, N.; et al. Detection of a SARS-CoV-2 variant of concern in South Africa. *Nature* **2021**, *592*, 438–443. [CrossRef] [PubMed]

44. Edara, V.V.; Pinsky, B.A.; Suthar, M.S.; Lai, L.; Davis-Gardner, M.E.; Floyd, K.; Flowers, M.W.; Wrammert, J.; Hussaini, L.; Ciric, C.R.; et al. Infection and Vaccine-Induced Neutralizing-Antibody Responses to the SARS-CoV-2 B.1.617 Variants. *N. Engl. J. Med.* **2021**, *385*, 664–666. [CrossRef]

45. McCallum, M.; Bassi, J.; De Marco, A.; Chen, A.; Walls, A.C.; Di Iulio, J.; Tortorici, M.A.; Navarro, M.J.; Silacci-Fregni, C.; Saliba, C.; et al. SARS-CoV-2 immune evasion by the B.1.427/B.1.429 variant of concern. *Science* **2021**, *373*, 648–654. [CrossRef]

46. Wang, P.; Nair, M.S.; Liu, L.; Iketani, S.; Luo, Y.; Guo, Y.; Wang, M.; Yu, J.; Zhang, B.; Kwong, P.D.; et al. Antibody resistance of SARS-CoV-2 variants B.1.351 and B.1.1.7. *Nature* **2021**, *593*, 130–135. [CrossRef]

47. Greaney, A.J.; Loes, A.N.; Crawford, K.H.D.; Starr, T.N.; Malone, K.D.; Chu, H.Y.; Bloom, J.D. Comprehensive mapping of mutations in the SARS-CoV-2 receptor-binding domain that affect recognition by polyclonal human plasma antibodies. *Cell Host Microbe* **2021**, *29*, 463–476.e6. [CrossRef]

48. Viana, R.; Moyo, S.; Amoako, D.G.; Tegally, H.; Scheepers, C.; Althaus, C.L.; Anyaneji, U.J.; Bester, P.A.; Boni, M.F.; Chand, M.; et al. Rapid epidemic expansion of the SARS-CoV-2 Omicron variant in southern Africa. *Nature* **2022**. [CrossRef]

49. European Centre for Disease Prevention and Control. *Implications of the Emergence and Spread of the SARSCoV-2 B.1.1.529 Variant of Concern (Omicron), for the EU/EEA*; ECDC: Stockholm, Sweden, 2021.

50. Andrews, N.; Stowe, J.; Kirsebom, F.; Toffa, S.; Tim Rickeard, T.; Gallagher, E.; Gower, C.; Kall, M.; Groves, N.; O'Connell, A.-M.; et al. Effectiveness of COVID-19 vaccines against the Omicron (B.1.1.529) variant of concern. *medRxiv* **2021**. [CrossRef]

51. Doria-Rose, N.A.; Shen, X.; Schmidt, S.D.; O'Dell, S.; McDanal, C.; Feng, W.; Tong, J.; Eaton, A.; Maglinao, M.; Tang, H.; et al. Booster of mRNA-1273 Strengthens SARS-CoV-2 Omicron Neutralization. *medRxiv* **2021**. [CrossRef]

52. Meng, B.; Abdullahi, A.; Ferreira, I.A.T.M.; Goonawardane, N.; Saito, A.; Kimura, I.; Yamasoba, D.; Gerba, P.P.; Fatihi, S.; Rathore, S.; et al. Altered TMPRSS2 usage by SARS-CoV-2 Omicron impacts tropism and fusogenisity. *Nature* **2022**. [CrossRef]

53. Ferguson, N.; Ghani, A.; Cori, A.; Hogan, A.; Hinsley, W.; Volz, E. *Growth, Population Distribution and Immune Escape of the Omicron in England*; Imperial College London: London, UK, 2021. [CrossRef]

54. Katelaris, A.L.; Wells, J.; Clark, P.; Norton, S.; Rockett, R.; Arnott, A.; Sintchenko, V.; Corbett, S.; Bag, S.K. Epidemiologic Evidence for Airborne Transmission of SARS-CoV-2 during Church Singing, Australia, 2020. *Emerg. Infect. Dis.* **2021**, *27*, 1677–1680. [CrossRef] [PubMed]

55. Marques, M.; Domingo, J.L. Contamination of inert surfaces by SARS-CoV-2: Persistence, stability and infectivity—A review. *Environ. Res.* **2021**, *193*, 110559. [CrossRef] [PubMed]

56. Meyerowitz, E.A.; Richterman, A.; Gandhi, R.T.; Sax, P.E. Transmission of SARS-CoV-2: A Review of Viral, Host, and Environmental Factors. *Ann. Intern. Med.* **2021**, *174*, 69–79. [CrossRef] [PubMed]

57. Zhang, X.S.; Duchaine, C. SARS-CoV-2 and Health Care Worker Protection in Low-Risk Settings: A Review of Modes of Transmission and a Novel Airborne Model Involving Inhalable Particles. *Clin. Microbiol. Rev.* **2020**, *34*, e00184-20. [CrossRef]

58. Bar-On, Y.M.; Flamholz, A.; Phillips, R.; Milo, R. SARS-CoV-2 (COVID-19) by the numbers. *eLife* **2020**, *9*, e57309. [CrossRef]

59. Campbell, F.; Archer, B.; Laurenson-Schafer, H.; Jinnai, Y.; Konings, F.; Batra, N.; Pavlin, B.; Vandemaele, K.; Van Kerkhove, M.D.; Jombart, T.; et al. Increased transmissibility and global spread of SARS-CoV-2 variants of concern as at June 2021. *Euro Surveill* **2021**, *26*, 2100509. [CrossRef]

60. Nishiura, H.; Ito, K.; Anzai, A.; Kobayashi, T.; Piantham, C.; Rodriguez-Morales, A.J. Relative Reproduction Number of SARS-CoV-2 Omicron (B.1.1.529) Compared with Delta Variant in South Africa. *J. Clin. Med.* **2021**, *11*, 30. [CrossRef]

61. Quesada, J.A.; Lopez-Pineda, A.; Gil-Guillen, V.F.; Arriero-Marin, J.M.; Gutierrez, F.; Carratala-Munuera, C. Incubation period of COVID-19: A systematic review and meta-analysis. *Rev. Clin. Esp.* **2021**, *221*, 109–117. [CrossRef]

62. Elias, C.; Sekri, A.; Leblanc, P.; Cucherat, M.; Vanhems, P. The incubation period of COVID-19: A meta-analysis. *Int. J. Infect. Dis.* **2021**, *104*, 708–710. [CrossRef]

63. Jansen, L.; Tegomoh, B.; Lange, K.; Showalter, K.; Figliomeni, J.; Abdalhamid, B.; Iwen, P.C.; Fauver, J.; Buss, B.; Donahue, M. Investigation of a SARS-CoV-2 B.1.1.529 (Omicron) Variant Cluster—Nebraska, November–December 2021. *MMWR Morb. Mortal. Wkly. Rep.* **2021**, *70*, 1782–1784. [CrossRef] [PubMed]

64. Buitrago-Garcia, D.; Egli-Gany, D.; Counotte, M.J.; Hossmann, S.; Imeri, H.; Ipekci, A.M.; Salanti, G.; Low, N. Occurrence and transmission potential of asymptomatic and presymptomatic SARS-CoV-2 infections: A living systematic review and meta-analysis. *PLoS Med.* **2020**, *17*, e1003346. [CrossRef] [PubMed]

65. Syangtan, G.; Bista, S.; Dawadi, P.; Rayamajhee, B.; Shrestha, L.B.; Tuladhar, R.; Joshi, D.R. Asymptomatic SARS-CoV-2 Carriers: A Systematic Review and Meta-Analysis. *Front. Public Health* **2020**, *8*, 587374. [CrossRef] [PubMed]

66. Wei, W.E.; Li, Z.; Chiew, C.J.; Yong, S.E.; Toh, M.P.; Lee, V.J. Presymptomatic Transmission of SARS-CoV-2—Singapore, January 23–March 16, 2020. *MMWR Morb. Mortal. Wkly. Rep.* **2020**, *69*, 411–415. [CrossRef] [PubMed]

67. Cevik, M.; Tate, M.; Lloyd, O.; Maraolo, A.E.; Schafers, J.; Ho, A. SARS-CoV-2, SARS-CoV, and MERS-CoV viral load dynamics, duration of viral shedding, and infectiousness: A systematic review and meta-analysis. *Lancet Microbe* **2021**, *2*, e13–e22. [CrossRef]

68. Qiu, X.; Nergiz, A.I.; Maraolo, A.E.; Bogoch, I.I.; Low, N.; Cevik, M. The role of asymptomatic and pre-symptomatic infection in SARS-CoV-2 transmission-a living systematic review. *Clin. Microbiol. Infect.* **2021**, *27*, 511–519. [CrossRef] [PubMed]

69. Li, B.; Deng, A.; Li, K.; Hu, Y.; Li, Z.; Shi, Y.; Xiong, Q.; Liu, Z.; Guo, Q.; Zou, L.; et al. Viral infection and transmission in a large, well-traced outbreak caused by the SARS-CoV-2 Delta variant. *Nat. Commun.* **2022**, *13*, 460. [CrossRef]

70. Torjesen, I. Covid-19: Peak of viral shedding is later with omicron variant, Japanese data suggest. *BMJ* **2022**, *376*, o89. [CrossRef]

71. Wadman, M.; Couzin-Frankel, J.; Kaiser, J.; Matacic, C. A rampage through the body. *Science* **2020**, *368*, 356–360. [CrossRef]

72. Eythorsson, E.; Helgason, D.; Ingvarsson, R.F.; Bjornsson, H.K.; Olafsdottir, L.B.; Bjarnadottir, V.; Runolfsdottir, H.L.; Bjarnadottir, S.; Agustsson, A.S.; Oskarsdottir, K.; et al. Clinical spectrum of coronavirus disease 2019 in Iceland: Population based cohort study. *BMJ* **2020**, *371*, m4529. [CrossRef]

73. Fisman, D.N.; Tuite, A.R. Evaluation of the relative virulence of novel SARS-CoV-2 variants: A retrospective cohort study in Ontario, Canada. *CMAJ* **2021**, *193*, E1619–E1625. [CrossRef] [PubMed]

74. Twohig, K.A.; Nyberg, T.; Zaidi, A.; Thelwall, S.; Sinnathamby, M.A.; Aliabadi, S.; Seaman, S.R.; Harris, R.J.; Hope, R.; Lopez-Bernal, J.; et al. Hospital admission and emergency care attendance risk for SARS-CoV-2 delta (B.1.617.2) compared with alpha (B.1.1.7) variants of concern: A cohort study. *Lancet Infect. Dis.* **2022**, *22*, 35–42. [CrossRef]

75. Post, N.; Eddy, D.; Huntley, C.; van Schalkwyk, M.C.I.; Shrotri, M.; Leeman, D.; Rigby, S.; Williams, S.V.; Bermingham, W.H.; Kellam, P.; et al. Antibody response to SARS-CoV-2 infection in humans: A systematic review. *PLoS ONE* **2020**, *15*, e0244126. [CrossRef] [PubMed]

76. Siordia, J.A., Jr. Epidemiology and clinical features of COVID-19: A review of current literature. *J. Clin. Virol.* **2020**, *127*, 104357. [CrossRef]

77. Osada, N.; Kohara, A.; Yamaji, T.; Hirayama, N.; Kasai, F.; Sekizuka, T.; Kuroda, M.; Hanada, K. The genome landscape of the african green monkey kidney-derived vero cell line. *DNA Res.* **2014**, *21*, 673–683. [CrossRef]

78. Desmyter, J.; Melnick, J.L.; Rawls, W.E. Defectiveness of interferon production and of rubella virus interference in a line of African green monkey kidney cells (Vero). *J. Virol.* **1968**, *2*, 955–961. [CrossRef] [PubMed]

79. Lau, S.Y.; Wang, P.; Mok, B.W.; Zhang, A.J.; Chu, H.; Lee, A.C.; Deng, S.; Chen, P.; Chan, K.H.; Song, W.; et al. Attenuated SARS-CoV-2 variants with deletions at the S1/S2 junction. *Emerg. Microbes Infect.* **2020**, *9*, 837–842. [CrossRef]

80. Mykytyn, A.Z.; Breugem, T.I.; Riesebosch, S.; Schipper, D.; van den Doel, P.B.; Rottier, R.J.; Lamers, M.M.; Haagmans, B.L. SARS-CoV-2 entry into human airway organoids is serine protease-mediated and facilitated by the multibasic cleavage site. *eLife* **2021**, *10*, e64508. [CrossRef]

81. Lamers, M.M.; Mykytyn, A.Z.; Breugem, T.I.; Wang, Y.; Wu, D.C.; Riesebosch, S.; van den Doel, P.B.; Schipper, D.; Bestebroer, T.; Wu, N.C.; et al. Human airway cells prevent SARS-CoV-2 multibasic cleavage site cell culture adaptation. *eLife* **2021**, *10*, e66815. [CrossRef]

82. Daniel, V.C.; Marchionni, L.; Hierman, J.S.; Rhodes, J.T.; Devereux, W.L.; Rudin, C.M.; Yung, R.; Parmigiani, G.; Dorsch, M.; Peacock, C.D.; et al. A primary xenograft model of small-cell lung cancer reveals irreversible changes in gene expression imposed by culture in vitro. *Cancer Res.* **2009**, *69*, 3364–3373. [CrossRef]

83. Hale, B.G. Avoiding culture shock with the SARS-CoV-2 spike protein. *eLife* **2021**, *10*, e69496. [CrossRef]

84. Milewska, A.; Kula-Pacurar, A.; Wadas, J.; Suder, A.; Szczepanski, A.; Dabrowska, A.; Owczarek, K.; Marcello, A.; Ochman, M.; Stacel, T.; et al. Replication of Severe Acute Respiratory Syndrome Coronavirus 2 in Human Respiratory Epithelium. *J. Virol.* **2020**, *94*, e00957-20. [CrossRef] [PubMed]

85. Lamers, M.M.; Beumer, J.; van der Vaart, J.; Knoops, K.; Puschhof, J.; Breugem, T.I.; Ravelli, R.B.G.; Paul van Schayck, J.; Mykytyn, A.Z.; Duimel, H.Q.; et al. SARS-CoV-2 productively infects human gut enterocytes. *Science* **2020**, *369*, 50–54. [CrossRef] [PubMed]

86. Hou, Y.J.; Okuda, K.; Edwards, C.E.; Martinez, D.R.; Asakura, T.; Dinnon, K.H., 3rd; Kato, T.; Lee, R.E.; Yount, B.L.; Mascenik, T.M.; et al. SARS-CoV-2 Reverse Genetics Reveals a Variable Infection Gradient in the Respiratory Tract. *Cell* **2020**, *182*, 429–446.e14. [CrossRef] [PubMed]

87. Hikmet, F.; Mear, L.; Edvinsson, A.; Micke, P.; Uhlen, M.; Lindskog, C. The protein expression profile of ACE2 in human tissues. *Mol. Syst. Biol.* **2020**, *16*, e9610. [CrossRef]

88. Mulay, A.; Konda, B.; Garcia, G., Jr.; Yao, C.; Beil, S.; Villalba, J.M.; Koziol, C.; Sen, C.; Purkayastha, A.; Kolls, J.K.; et al. SARS-CoV-2 infection of primary human lung epithelium for COVID-19 modeling and drug discovery. *Cell Rep.* **2021**, *35*, 109055. [CrossRef]

89. Ravindra, N.G.; Alfajaro, M.M.; Gasque, V.; Huston, N.C.; Wan, H.; Szigeti-Buck, K.; Yasumoto, Y.; Greaney, A.M.; Habet, V.; Chow, R.D.; et al. Single-cell longitudinal analysis of SARS-CoV-2 infection in human airway epithelium identifies target cells, alterations in gene expression, and cell state changes. *PLoS Biol.* **2021**, *19*, e3001143. [CrossRef]

90. van der Vaart, J.; Lamers, M.M.; Haagmans, B.L.; Clevers, H. Advancing lung organoids for COVID-19 research. *Dis. Models Mech.* **2021**, *14*, dmm049060. [CrossRef]

91. Baldassi, D.; Gabold, B.; Merkel, O. Air-liquid interface cultures of the healthy and diseased human respiratory tract: Promises, challenges and future directions. *Adv. Nanobiomed. Res.* **2021**, *1*, 2000111. [CrossRef]

92. Egilmezer, E.; Rawlinson, W.D. Review of studies of severe acute respiratory syndrome related coronavirus-2 pathogenesis in human organoid models. *Rev. Med. Virol.* **2021**, *31*, e2227. [CrossRef]

93. Nabhan, A.N.; Brownfield, D.G.; Harbury, P.B.; Krasnow, M.A.; Desai, T.J. Single-cell Wnt signaling niches maintain stemness of alveolar type 2 cells. *Science* **2018**, *359*, 1118–1123. [CrossRef] [PubMed]

94. Zacharias, W.J.; Frank, D.B.; Zepp, J.A.; Morley, M.P.; Alkhaleel, F.A.; Kong, J.; Zhou, S.; Cantu, E.; Morrisey, E.E. Regeneration of the lung alveolus by an evolutionarily conserved epithelial progenitor. *Nature* **2018**, *555*, 251–255. [CrossRef] [PubMed]

95. van den Bogaard, E.H.; Dailey, L.A.; Thorley, A.J.; Tetley, T.D.; Forbes, B. Inflammatory response and barrier properties of a new alveolar type 1-like cell line (TT1). *Pharm. Res.* **2009**, *26*, 1172–1180. [CrossRef] [PubMed]

96. Lamers, M.M.; van der Vaart, J.; Knoops, K.; Riesebosch, S.; Breugem, T.I.; Mykytyn, A.Z.; Beumer, J.; Schipper, D.; Bezstarosti, K.; Koopman, C.D.; et al. An organoid-derived bronchioalveolar model for SARS-CoV-2 infection of human alveolar type II-like cells. *EMBO J.* **2021**, *40*, e105912. [CrossRef]

97. Gard, A.L.; Luu, R.J.; Miller, C.R.; Maloney, R.; Cain, B.P.; Marr, E.E.; Burns, D.M.; Gaibler, R.; Mulhern, T.J.; Wong, C.A.; et al. High-throughput human primary cell-based airway model for evaluating influenza, coronavirus, or other respiratory viruses in vitro. *Sci. Rep.* **2021**, *11*, 14961. [CrossRef]

98. Chen, K.G.; Park, K.; Spence, J.R. Studying SARS-CoV-2 infectivity and therapeutic responses with complex organoids. *Nat. Cell Biol.* **2021**, *23*, 822–833. [CrossRef]

99. Han, Y.; Duan, X.; Yang, L.; Nilsson-Payant, B.E.; Wang, P.; Duan, F.; Tang, X.; Yaron, T.M.; Zhang, T.; Uhl, S.; et al. Identification of SARS-CoV-2 inhibitors using lung and colonic organoids. *Nature* **2021**, *589*, 270–275. [CrossRef]

100. Barker, N.; van Es, J.H.; Kuipers, J.; Kujala, P.; van den Born, M.; Cozijnsen, M.; Haegebarth, A.; Korving, J.; Begthel, H.; Peters, P.J.; et al. Identification of stem cells in small intestine and colon by marker gene Lgr5. *Nature* **2007**, *449*, 1003–1007. [CrossRef]

101. Sato, T.; van Es, J.H.; Snippert, H.J.; Stange, D.E.; Vries, R.G.; van den Born, M.; Barker, N.; Shroyer, N.F.; van de Wetering, M.; Clevers, H. Paneth cells constitute the niche for Lgr5 stem cells in intestinal crypts. *Nature* **2011**, *469*, 415–418. [CrossRef]

102. Lamers, M.M.; Breugem, T.I.; Mykytyn, A.Z.; Wang, Y.; Groen, N.; Knoops, K.; Schipper, D.; van der Vaart, J.; Koopman, C.D.; Zhang, J.; et al. Human organoid systems reveal in vitro correlates of fitness for SARS-CoV-2 B.1.1.7. *bioRXiv* **2021**. [CrossRef]

103. Burgueno, J.F.; Reich, A.; Hazime, H.; Quintero, M.A.; Fernandez, I.; Fritsch, J.; Santander, A.M.; Brito, N.; Damas, O.M.; Deshpande, A.; et al. Expression of SARS-CoV-2 Entry Molecules ACE2 and TMPRSS2 in the Gut of Patients With IBD. *Inflamm. Bowel Dis.* **2020**, *26*, 797–808. [CrossRef] [PubMed]

104. Guo, M.; Tao, W.; Flavell, R.A.; Zhu, S. Potential intestinal infection and faecal-oral transmission of SARS-CoV-2. *Nat. Rev. Gastroenterol. Hepatol.* **2021**, *18*, 269–283. [CrossRef] [PubMed]

105. Zuo, T.; Zhang, F.; Lui, G.C.Y.; Yeoh, Y.K.; Li, A.Y.L.; Zhan, H.; Wan, Y.; Chung, A.C.K.; Cheung, C.P.; Chen, N.; et al. Alterations in Gut Microbiota of Patients With COVID-19 During Time of Hospitalization. *Gastroenterology* **2020**, *159*, 944–955. [CrossRef] [PubMed]

106. Bulfamante, G.P.; Perrucci, G.L.; Falleni, M.; Sommariva, E.; Tosi, D.; Martinelli, C.; Songia, P.; Poggio, P.; Carugo, S.; Pompilio, G. Evidence of SARS-CoV-2 Transcriptional Activity in Cardiomyocytes of COVID-19 Patients without Clinical Signs of Cardiac Involvement. *Biomedicines* **2020**, *8*, 626. [CrossRef]

107. Perez-Bermejo, J.A.; Kang, S.; Rockwood, S.J.; Simoneau, C.R.; Joy, D.A.; Silva, A.C.; Ramadoss, G.N.; Flanigan, W.R.; Fozouni, P.; Li, H.; et al. SARS-CoV-2 infection of human iPSC-derived cardiac cells reflects cytopathic features in hearts of patients with COVID-19. *Sci. Transl. Med.* **2021**, *13*, eafb7872. [CrossRef]

108. Williams, T.L.; Colzani, M.T.; Macrae, R.G.C.; Robinson, E.L.; Bloor, S.; Greenwood, E.J.D.; Zhan, J.R.; Strachan, G.; Kuc, R.E.; Nyimanu, D.; et al. Human embryonic stem cell-derived cardiomyocyte platform screens inhibitors of SARS-CoV-2 infection. *Commun. Biol.* **2021**, *4*, 926. [CrossRef]

109. Marchiano, S.; Hsiang, T.Y.; Khanna, A.; Higashi, T.; Whitmore, L.S.; Bargehr, J.; Davaapil, H.; Chang, J.; Smith, E.; Ong, L.P.; et al. SARS-CoV-2 Infects Human Pluripotent Stem Cell-Derived Cardiomyocytes, Impairing Electrical and Mechanical Function. *Stem Cell Rep.* **2021**, *16*, 478–492. [CrossRef]

110. Bojkova, D.; Wagner, J.U.G.; Shumliakivska, M.; Aslan, G.S.; Saleem, U.; Hansen, A.; Luxan, G.; Gunther, S.; Pham, M.D.; Krishnan, J.; et al. SARS-CoV-2 infects and induces cytotoxic effects in human cardiomyocytes. *Cardiovasc. Res.* **2020**, *116*, 2207–2215. [CrossRef]

111. Sharma, A.; Garcia, G., Jr.; Wang, Y.; Plummer, J.T.; Morizono, K.; Arumugaswami, V.; Svendsen, C.N. Human iPSC-Derived Cardiomyocytes Are Susceptible to SARS-CoV-2 Infection. *Cell Rep. Med.* **2020**, *1*, 100052. [CrossRef]

112. Garcia, G., Jr.; Sharma, A.; Ramaiah, A.; Sen, C.; Purkayastha, A.; Kohn, D.B.; Parcells, M.S.; Beck, S.; Kim, H.; Bakowski, M.A.; et al. Antiviral drug screen identifies DNA-damage response inhibitor as potent blocker of SARS-CoV-2 replication. *Cell Rep.* **2021**, *35*, 108940. [CrossRef]

113. Wang, Q.; Zhao, H.; Liu, L.G.; Wang, Y.B.; Zhang, T.; Li, M.H.; Xu, Y.L.; Gao, G.J.; Xiong, H.F.; Fan, Y.; et al. Pattern of liver injury in adult patients with COVID-19: A retrospective analysis of 105 patients. *Mil. Med. Res.* **2020**, *7*, 28. [CrossRef] [PubMed]

114. Qi, F.; Qian, S.; Zhang, S.; Zhang, Z. Single cell RNA sequencing of 13 human tissues identify cell types and receptors of human coronaviruses. *Biochem. Biophys. Res. Commun.* **2020**, *526*, 135–140. [CrossRef] [PubMed]

115. Seow, J.J.W.; Pai, R.; Mishra, A.; Shepherdson, E.; Lim, T.K.H.; Goh, B.K.P.; Chan, J.K.Y.; Chow, P.K.H.; Ginhoux, F.; DasGupta, R.; et al. Single-Cell RNA-seq Reveals Angiotensin-Converting Enzyme 2 and Transmembrane Serine Protease 2 Expression in TROP2$^+$ Liver Progenitor Cells: Implications in Coronavirus Disease 2019-Associated Liver Dysfunction. *Front. Med.* **2021**, *8*, 603374. [CrossRef]

116. Zhao, B.; Ni, C.; Gao, R.; Wang, Y.; Yang, L.; Wei, J.; Lv, T.; Liang, J.; Zhang, Q.; Xu, W.; et al. Recapitulation of SARS-CoV-2 infection and cholangiocyte damage with human liver ductal organoids. *Protein Cell* **2020**, *11*, 771–775. [CrossRef] [PubMed]

117. Huch, M.; Dorrell, C.; Boj, S.F.; van Es, J.H.; Li, V.S.; van de Wetering, M.; Sato, T.; Hamer, K.; Sasaki, N.; Finegold, M.J.; et al. In vitro expansion of single Lgr5+ liver stem cells induced by Wnt-driven regeneration. *Nature* **2013**, *494*, 247–250. [CrossRef]

118. Huch, M.; Gehart, H.; van Boxtel, R.; Hamer, K.; Blokzijl, F.; Verstegen, M.M.; Ellis, E.; van Wenum, M.; Fuchs, S.A.; de Ligt, J.; et al. Long-term culture of genome-stable bipotent stem cells from adult human liver. *Cell* **2015**, *160*, 299–312. [CrossRef]

119. McCarron, S.; Bathon, B.; Conlon, D.M.; Abbey, D.; Rader, D.J.; Gawronski, K.; Brown, C.D.; Olthoff, K.M.; Shaked, A.; Raabe, T.D. Functional Characterization of Organoids Derived From Irreversibly Damaged Liver of Patients With NASH. *Hepatology* **2021**, *74*, 1825–1844. [CrossRef]

120. Targher, G.; Mantovani, A.; Byrne, C.D.; Wang, X.B.; Yan, H.D.; Sun, Q.F.; Pan, K.H.; Zheng, K.I.; Chen, Y.P.; Eslam, M.; et al. Risk of severe illness from COVID-19 in patients with metabolic dysfunction-associated fatty liver disease and increased fibrosis scores. *Gut* **2020**, *69*, 1545–1547. [CrossRef]

121. Mao, L.; Jin, H.; Wang, M.; Hu, Y.; Chen, S.; He, Q.; Chang, J.; Hong, C.; Zhou, Y.; Wang, D.; et al. Neurologic Manifestations of Hospitalized Patients With Coronavirus Disease 2019 in Wuhan, China. *JAMA Neurol.* **2020**, *77*, 683–690. [CrossRef]

122. Lu, Y.; Li, X.; Geng, D.; Mei, N.; Wu, P.Y.; Huang, C.C.; Jia, T.; Zhao, Y.; Wang, D.; Xiao, A.; et al. Cerebral Micro-Structural Changes in COVID-19 Patients—An MRI-based 3-month Follow-up Study. *EClinicalMedicine* **2020**, *25*, 100484. [CrossRef]

123. Ellul, M.A.; Benjamin, L.; Singh, B.; Lant, S.; Michael, B.D.; Easton, A.; Kneen, R.; Defres, S.; Sejvar, J.; Solomon, T. Neurological associations of COVID-19. *Lancet Neurol.* **2020**, *19*, 767–783. [CrossRef]

124. Edler, C.; Schroder, A.S.; Aepfelbacher, M.; Fitzek, A.; Heinemann, A.; Heinrich, F.; Klein, A.; Langenwalder, F.; Lutgehetmann, M.; Meissner, K.; et al. Dying with SARS-CoV-2 infection-an autopsy study of the first consecutive 80 cases in Hamburg, Germany. *Int. J. Legal Med.* **2020**, *134*, 1275–1284. [CrossRef] [PubMed]

125. Ramani, A.; Muller, L.; Ostermann, P.N.; Gabriel, E.; Abida-Islam, P.; Muller-Schiffmann, A.; Mariappan, A.; Goureau, O.; Gruell, H.; Walker, A.; et al. SARS-CoV-2 targets neurons of 3D human brain organoids. *EMBO J.* **2020**, *39*, e106230. [CrossRef]

126. Jacob, F.; Pather, S.R.; Huang, W.K.; Zhang, F.; Wong, S.Z.H.; Zhou, H.; Cubitt, B.; Fan, W.; Chen, C.Z.; Xu, M.; et al. Human Pluripotent Stem Cell-Derived Neural Cells and Brain Organoids Reveal SARS-CoV-2 Neurotropism Predominates in Choroid Plexus Epithelium. *Cell Stem Cell* **2020**, *27*, 937–950. [CrossRef] [PubMed]

127. Pellegrini, L.; Albecka, A.; Mallery, D.L.; Kellner, M.J.; Paul, D.; Carter, A.P.; James, L.C.; Lancaster, M.A. SARS-CoV-2 Infects the Brain Choroid Plexus and Disrupts the Blood-CSF Barrier in Human Brain Organoids. *Cell Stem Cell* **2020**, *27*, 951–961. [CrossRef] [PubMed]

128. Meinhardt, J.; Radke, J.; Dittmayer, C.; Franz, J.; Thomas, C.; Mothes, R.; Laue, M.; Schneider, J.; Brunink, S.; Greuel, S.; et al. Olfactory transmucosal SARS-CoV-2 invasion as a port of central nervous system entry in individuals with COVID-19. *Nat. Neurosci.* **2021**, *24*, 168–175. [CrossRef]

129. Danilczyk, U.; Penninger, J.M. Angiotensin-converting enzyme II in the heart and the kidney. *Circ. Res.* **2006**, *98*, 463–471. [CrossRef]

130. Lin, W.; Fan, J.; Hu, L.F.; Zhang, Y.; Ooi, J.D.; Meng, T.; Jin, P.; Ding, X.; Peng, L.K.; Song, L.; et al. Single-cell analysis of angiotensin-converting enzyme II expression in human kidneys and bladders reveals a potential route of 2019 novel coronavirus infection. *Chin. Med. J.* **2021**, *134*, 935–943. [CrossRef]

131. Ling, Y.; Xu, S.B.; Lin, Y.X.; Tian, D.; Zhu, Z.Q.; Dai, F.H.; Wu, F.; Song, Z.G.; Huang, W.; Chen, J.; et al. Persistence and clearance of viral RNA in 2019 novel coronavirus disease rehabilitation patients. *Chin. Med. J.* **2020**, *133*, 1039–1043. [CrossRef]

132. Braun, F.; Lutgehetmann, M.; Pfefferle, S.; Wong, M.N.; Carsten, A.; Lindenmeyer, M.T.; Norz, D.; Heinrich, F.; Meissner, K.; Wichmann, D.; et al. SARS-CoV-2 renal tropism associates with acute kidney injury. *Lancet* **2020**, *396*, 597–598. [CrossRef]

133. Caceres, P.S.; Savickas, G.; Murray, S.L.; Umanath, K.; Uduman, J.; Yee, J.; Liao, T.D.; Bolin, S.; Levin, A.M.; Khan, M.N.; et al. High SARS-CoV-2 Viral Load in Urine Sediment Correlates with Acute Kidney Injury and Poor COVID-19 Outcome. *J. Am. Soc. Nephrol.* **2021**, *32*, 2517–2528. [CrossRef]

134. Ahmadian, E.; Hosseiniyan Khatibi, S.M.; Razi Soofiyani, S.; Abediazar, S.; Shoja, M.M.; Ardalan, M.; Zununi Vahed, S. Covid-19 and kidney injury: Pathophysiology and molecular mechanisms. *Rev. Med. Virol.* **2021**, *31*, e2176. [CrossRef]

135. Gabarre, P.; Dumas, G.; Dupont, T.; Darmon, M.; Azoulay, E.; Zafrani, L. Acute kidney injury in critically ill patients with COVID-19. *Intensive Care Med.* **2020**, *46*, 1339–1348. [CrossRef]

136. Monteil, V.; Kwon, H.; Prado, P.; Hagelkruys, A.; Wimmer, R.A.; Stahl, M.; Leopoldi, A.; Garreta, E.; Hurtado Del Pozo, C.; Prosper, F.; et al. Inhibition of SARS-CoV-2 Infections in Engineered Human Tissues Using Clinical-Grade Soluble Human ACE2. *Cell* **2020**, *181*, 905–913. [CrossRef]

137. Wysocki, J.; Ye, M.; Hassler, L.; Gupta, A.K.; Wang, Y.; Nicoleascu, V.; Randall, G.; Wertheim, J.A.; Batlle, D. A Novel Soluble ACE2 Variant with Prolonged Duration of Action Neutralizes SARS-CoV-2 Infection in Human Kidney Organoids. *J. Am. Soc. Nephrol.* **2021**, *32*, 795–803. [CrossRef]

138. Monteil, V.; Dyczynski, M.; Lauschke, V.M.; Kwon, H.; Wirnsberger, G.; Youhanna, S.; Zhang, H.; Slutsky, A.S.; Hurtado Del Pozo, C.; Horn, M.; et al. Human soluble ACE2 improves the effect of remdesivir in SARS-CoV-2 infection. *EMBO Mol. Med.* **2021**, *13*, e13426. [CrossRef]

139. Xia, S.; Wu, M.; Chen, S.; Zhang, T.; Ye, L.; Liu, J.; Li, H. Long Term Culture of Human Kidney Proximal Tubule Epithelial Cells Maintains Lineage Functions and Serves as an Ex vivo Model for Coronavirus Associated Kidney Injury. *Virol. Sin.* **2020**, *35*, 311–320. [CrossRef]

140. Liu, X.; Krawczyk, E.; Suprynowicz, F.A.; Palechor-Ceron, N.; Yuan, H.; Dakic, A.; Simic, V.; Zheng, Y.L.; Sripadhan, P.; Chen, C.; et al. Conditional reprogramming and long-term expansion of normal and tumor cells from human biospecimens. *Nat. Protoc.* **2017**, *12*, 439–451. [CrossRef]

141. Lu, C.W.; Liu, X.F.; Jia, Z.F. 2019-nCoV transmission through the ocular surface must not be ignored. *Lancet* **2020**, *395*, e39. [CrossRef]

142. Eriksen, A.Z.; Moller, R.; Makovoz, B.; Uhl, S.A.; tenOever, B.R.; Blenkinsop, T.A. SARS-CoV-2 infects human adult donor eyes and hESC-derived ocular epithelium. *Cell Stem Cell* **2021**, *28*, 1205–1220. [CrossRef]

143. Zhou, L.; Xu, Z.; Castiglione, G.M.; Soiberman, U.S.; Eberhart, C.G.; Duh, E.J. ACE2 and TMPRSS2 are expressed on the human ocular surface, suggesting susceptibility to SARS-CoV-2 infection. *Ocul. Surf.* **2020**, *18*, 537–544. [CrossRef] [PubMed]

144. Cowan, C.S.; Renner, M.; De Gennaro, M.; Gross-Scherf, B.; Goldblum, D.; Hou, Y.; Munz, M.; Rodrigues, T.M.; Krol, J.; Szikra, T.; et al. Cell Types of the Human Retina and Its Organoids at Single-Cell Resolution. *Cell* **2020**, *182*, 1623–1640. [CrossRef]

145. Makovoz, B.; Moeller, R.; Zebitz Eriksen, A.; tenOever, B.R.; Blenkinsop, T.A. SARS-CoV-2 Infection of Ocular Cells from Human Adult Donor Eyes and hESC-Derived Eye Organoids. *SSRN* **2020**, 3650574. [CrossRef]

146. Ahmad Mulyadi Lai, H.I.; Chou, S.J.; Chien, Y.; Tsai, P.H.; Chien, C.S.; Hsu, C.C.; Jheng, Y.C.; Wang, M.L.; Chiou, S.H.; Chou, Y.B.; et al. Expression of Endogenous Angiotensin-Converting Enzyme 2 in Human Induced Pluripotent Stem Cell-Derived Retinal Organoids. *Int. J. Mol. Sci.* **2021**, *22*, 1320. [CrossRef]

147. Flaumenhaft, R.; Enjyoji, K.; Schmaier, A.A. Vasculopathy in COVID-19. *Blood* **2022**. [CrossRef]

148. Ruhl, L.; Pink, I.; Kuhne, J.F.; Beushausen, K.; Keil, J.; Christoph, S.; Sauer, A.; Boblitz, L.; Schmidt, J.; David, S.; et al. Endothelial dysfunction contributes to severe COVID-19 in combination with dysregulated lymphocyte responses and cytokine networks. *Signal Transduct. Target. Ther.* **2021**, *6*, 418. [CrossRef]

149. Pons, S.; Fodil, S.; Azoulay, E.; Zafrani, L. The vascular endothelium: The cornerstone of organ dysfunction in severe SARS-CoV-2 infection. *Crit. Care* **2020**, *24*, 353. [CrossRef]

150. Huertas, A.; Montani, D.; Savale, L.; Pichon, J.; Tu, L.; Parent, F.; Guignabert, C.; Humbert, M. Endothelial cell dysfunction: A major player in SARS-CoV-2 infection (COVID-19)? *Eur. Respir. J.* **2020**, *56*. [CrossRef]

151. Jin, Y.; Ji, W.; Yang, H.; Chen, S.; Zhang, W.; Duan, G. Endothelial activation and dysfunction in COVID-19: From basic mechanisms to potential therapeutic approaches. *Signal Transduct. Target. Ther.* **2020**, *5*, 293. [CrossRef]

152. Guervilly, C.; Burtey, S.; Sabatier, F.; Cauchois, R.; Lano, G.; Abdili, E.; Daviet, F.; Arnaud, L.; Brunet, P.; Hraiech, S.; et al. Circulating Endothelial Cells as a Marker of Endothelial Injury in Severe COVID-19. *J. Infect. Dis.* **2020**, *222*, 1789–1793. [CrossRef]

153. Nizzoli, M.E.; Merati, G.; Tenore, A.; Picone, C.; Consensi, E.; Perotti, L.; Ferretti, V.V.; Sambo, M.; Di Sabatino, A.; Iotti, G.A.; et al. Circulating endothelial cells in COVID-19. *Am. J. Hematol.* **2020**, *95*, E187–E188. [CrossRef] [PubMed]

154. Varga, Z.; Flammer, A.J.; Steiger, P.; Haberecker, M.; Andermatt, R.; Zinkernagel, A.S.; Mehra, M.R.; Schuepbach, R.A.; Ruschitzka, F.; Moch, H. Endothelial cell infection and endotheliitis in COVID-19. *Lancet* **2020**, *395*, 1417–1418. [CrossRef]

155. Yang, L.; Han, Y.; Nilsson-Payant, B.E.; Gupta, V.; Wang, P.; Duan, X.; Tang, X.; Zhu, J.; Zhao, Z.; Jaffre, F.; et al. A Human Pluripotent Stem Cell-based Platform to Study SARS-CoV-2 Tropism and Model Virus Infection in Human Cells and Organoids. *Cell Stem Cell* **2020**, *27*, 125–136. [CrossRef] [PubMed]

156. Liu, F.; Han, K.; Blair, R.; Kenst, K.; Qin, Z.; Upcin, B.; Worsdorfer, P.; Midkiff, C.C.; Mudd, J.; Belyaeva, E.; et al. SARS-CoV-2 Infects Endothelial Cells in Vivo and in Vitro. *Front. Cell Infect. Microbiol.* **2021**, *11*, 701278. [CrossRef] [PubMed]

157. Schimmel, L.; Chew, K.Y.; Stocks, C.J.; Yordanov, T.E.; Essebier, P.; Kulasinghe, A.; Monkman, J.; Dos Santos Miggiolaro, A.F.R.; Cooper, C.; de Noronha, L.; et al. Endothelial cells are not productively infected by SARS-CoV-2. *Clin. Transl. Immunol.* **2021**, *10*, e1350. [CrossRef]

158. Wagner, J.U.G.; Bojkova, D.; Shumliakivska, M.; Luxan, G.; Nicin, L.; Aslan, G.S.; Milting, H.; Kandler, J.D.; Dendorfer, A.; Heumueller, A.W.; et al. Increased susceptibility of human endothelial cells to infections by SARS-CoV-2 variants. *Basic Res. Cardiol.* **2021**, *116*, 42. [CrossRef]

159. Rauti, R.; Shahoha, M.; Leichtmann-Bardoogo, Y.; Nasser, R.; Paz, E.; Tamir, R.; Miller, V.; Babich, T.; Shaked, K.; Ehrlich, A.; et al. Effect of SARS-CoV-2 proteins on vascular permeability. *eLife* **2021**, *10*, e69314. [CrossRef]

160. Takasato, M.; Er, P.X.; Chiu, H.S.; Maier, B.; Baillie, G.J.; Ferguson, C.; Parton, R.G.; Wolvetang, E.J.; Roost, M.S.; Chuva de Sousa Lopes, S.M.; et al. Kidney organoids from human iPS cells contain multiple lineages and model human nephrogenesis. *Nature* **2015**, *526*, 564–568. [CrossRef]
161. Belhadjer, Z.; Meot, M.; Bajolle, F.; Khraiche, D.; Legendre, A.; Abakka, S.; Auriau, J.; Grimaud, M.; Oualha, M.; Beghetti, M.; et al. Acute Heart Failure in Multisystem Inflammatory Syndrome in Children in the Context of Global SARS-CoV-2 Pandemic. *Circulation* **2020**, *142*, 429–436. [CrossRef]
162. Chiotos, K.; Bassiri, H.; Behrens, E.M.; Blatz, A.M.; Chang, J.; Diorio, C.; Fitzgerald, J.C.; Topjian, A.; John, A.R.O. Multisystem Inflammatory Syndrome in Children During the Coronavirus 2019 Pandemic: A Case Series. *J. Pediatr. Infect. Dis. Soc.* **2020**, *9*, 393–398. [CrossRef]
163. Dufort, E.M.; Koumans, E.H.; Chow, E.J.; Rosenthal, E.M.; Muse, A.; Rowlands, J.; Barranco, M.A.; Maxted, A.M.; Rosenberg, E.S.; Easton, D.; et al. Multisystem Inflammatory Syndrome in Children in New York State. *N. Engl. J. Med.* **2020**, *383*, 347–358. [CrossRef] [PubMed]
164. Rauf, A.; Vijayan, A.; John, S.T.; Krishnan, R.; Latheef, A. Multisystem Inflammatory Syndrome with Features of Atypical Kawasaki Disease during COVID-19 Pandemic. *Indian J. Pediatr.* **2020**, *87*, 745–747. [CrossRef] [PubMed]
165. DeBiasi, R.L.; Song, X.; Delaney, M.; Bell, M.; Smith, K.; Pershad, J.; Ansusinha, E.; Hahn, A.; Hamdy, R.; Harik, N.; et al. Severe Coronavirus Disease-2019 in Children and Young Adults in the Washington, DC, Metropolitan Region. *J. Pediatr.* **2020**, *223*, 199–203. [CrossRef] [PubMed]
166. Lee, P.Y.; Day-Lewis, M.; Henderson, L.A.; Friedman, K.G.; Lo, J.; Roberts, J.E.; Lo, M.S.; Platt, C.D.; Chou, J.; Hoyt, K.J.; et al. Distinct clinical and immunological features of SARS-CoV-2-induced multisystem inflammatory syndrome in children. *J. Clin. Investig.* **2020**, *130*, 5942–5950. [CrossRef] [PubMed]
167. Tang, N.; Bai, H.; Chen, X.; Gong, J.; Li, D.; Sun, Z. Anticoagulant treatment is associated with decreased mortality in severe coronavirus disease 2019 patients with coagulopathy. *J. Thromb. Haemost.* **2020**, *18*, 1094–1099. [CrossRef]
168. Paranjpe, I.; Fuster, V.; Lala, A.; Russak, A.J.; Glicksberg, B.S.; Levin, M.A.; Charney, A.W.; Narula, J.; Fayad, Z.A.; Bagiella, E.; et al. Association of Treatment Dose Anticoagulation With In-Hospital Survival Among Hospitalized Patients With COVID-19. *J. Am. Coll. Cardiol.* **2020**, *76*, 122–124. [CrossRef]
169. Charfeddine, S.; Ibn Hadj Amor, H.; Jdidi, J.; Torjmen, S.; Kraiem, S.; Hammami, R.; Bahloul, A.; Kallel, N.; Moussa, N.; Touil, I.; et al. Long COVID 19 Syndrome: Is It Related to Microcirculation and Endothelial Dysfunction? Insights From TUN-EndCOV Study. *Front. Cardiovasc. Med.* **2021**, *8*, 745758. [CrossRef]
170. Zhang, Y.Z.; Holmes, E.C. A Genomic Perspective on the Origin and Emergence of SARS-CoV-2. *Cell* **2020**, *181*, 223–227. [CrossRef]
171. OIE. COVID-19—Events in Animals. 2021. Available online: https://www.oie.int/en/scientific-expertise/specific-information-and-recommendations/questions-and-answers-on-2019novel-coronavirus/events-in-animals (accessed on 28 January 2022).
172. Sooksawasdi Na Ayudhya, S.; Kuiken, T. Reverse Zoonosis of COVID-19: Lessons From the 2009 Influenza Pandemic. *Vet. Pathol.* **2021**, *58*, 234–242. [CrossRef]
173. Farag, E.A.; Islam, M.M.; Enan, K.; El-Hussein, A.M.; Bansal, D.; Haroun, M. SARS-CoV-2 at the human-animal interphase: A review. *Heliyon* **2021**, *7*, e08496. [CrossRef]
174. Goraichuk, I.V.; Arefiev, V.; Stegniy, B.T.; Gerilovych, A.P. Zoonotic and Reverse Zoonotic Transmissibility of SARS-CoV-2. *Virus Res.* **2021**, *302*, 198473. [CrossRef] [PubMed]
175. Jo, W.K.; de Oliveira-Filho, E.F.; Rasche, A.; Greenwood, A.D.; Osterrieder, K.; Drexler, J.F. Potential zoonotic sources of SARS-CoV-2 infections. *Transbound. Emerg. Dis.* **2021**, *68*, 1824–1834. [CrossRef] [PubMed]
176. de Morais, H.A.; Dos Santos, A.P.; do Nascimento, N.C.; Kmetiuk, L.B.; Barbosa, D.S.; Brandao, P.E.; Guimaraes, A.M.S.; Pettan-Brewer, C.; Biondo, A.W. Natural Infection by SARS-CoV-2 in Companion Animals: A Review of Case Reports and Current Evidence of Their Role in the Epidemiology of COVID-19. *Front. Vet. Sci.* **2020**, *7*, 591216. [CrossRef] [PubMed]
177. Garigliany, M.; Van Laere, A.S.; Clercx, C.; Giet, D.; Escriou, N.; Huon, C.; van der Werf, S.; Eloit, M.; Desmecht, D. SARS-CoV-2 Natural Transmission from Human to Cat, Belgium, March 2020. *Emerg. Infect. Dis.* **2020**, *26*, 3069–3071. [CrossRef] [PubMed]
178. Sit, T.H.C.; Brackman, C.J.; Ip, S.M.; Tam, K.W.S.; Law, P.Y.T.; To, E.M.W.; Yu, V.Y.T.; Sims, L.D.; Tsang, D.N.C.; Chu, D.K.W.; et al. Infection of dogs with SARS-CoV-2. *Nature* **2020**, *586*, 776–778. [CrossRef] [PubMed]
179. Gortazar, C.; Barroso-Arevalo, S.; Ferreras-Colino, E.; Isla, J.; de la Fuente, G.; Rivera, B.; Dominguez, L.; de la Fuente, J.; Sanchez-Vizcaino, J.M. Natural SARS-CoV-2 Infection in Kept Ferrets, Spain. *Emerg. Infect. Dis.* **2021**, *27*, 1994–1996. [CrossRef] [PubMed]
180. Giner, J.; Villanueva-Saz, S.; Tobajas, A.P.; Perez, M.D.; Gonzalez, A.; Verde, M.; Yzuel, A.; Garcia-Garcia, A.; Taleb, V.; Lira-Navarrete, E.; et al. SARS-CoV-2 Seroprevalence in Household Domestic Ferrets (Mustela putorius furo). *Animals* **2021**, *11*, 667. [CrossRef]
181. Halfmann, P.J.; Hatta, M.; Chiba, S.; Maemura, T.; Fan, S.; Takeda, M.; Kinoshita, N.; Hattori, S.I.; Sakai-Tagawa, Y.; Iwatsuki-Horimoto, K.; et al. Transmission of SARS-CoV-2 in Domestic Cats. *N. Engl. J. Med.* **2020**, *383*, 592–594. [CrossRef]
182. McAloose, D.; Laverack, M.; Wang, L.; Killian, M.L.; Caserta, L.C.; Yuan, F.; Mitchell, P.K.; Queen, K.; Mauldin, M.R.; Cronk, B.D.; et al. From People to Panthera: Natural SARS-CoV-2 Infection in Tigers and Lions at the Bronx Zoo. *mBio* **2020**, *11*, e02220-20. [CrossRef]

183. USDA. USDA Statement on the Confirmation of COVID-19 in a Tiger in New York. 2020. Available online: https://www.aphis. usda.gov/aphis/newsroom/news/sa_by_date/sa-2020/ny-zoo-covid-2019 (accessed on 1 February 2022).

184. OIE. COVID-19 Update (356): South Africa (GT) Animal, Puma, Zoo. 2020. Available online: https://promedmail.org/promed-post/?id=20200813.27673666 (accessed on 3 February 2022).

185. USDA; APHIS. Confirmation of COVID-19 in Snow Leopard at Kentucky Zoo. 2020. Available online: https://www.aphis.usda. gov/aphis/newsroom/stakeholder-info/sa_by_date/sa-2020/sa-2012/ky-snow-leopard-covid (accessed on 3 February 2022).

186. Gibbons, A. Captive Gorillas Test Positive for Coronavirus. 2021. Available online: https://pulitzercenter.org/stories/captive-gorillas-test-positive-coronavirus (accessed on 1 February 2022).

187. USDA; APHIS. Confirmation of COVID-19 in Gorillas at a California Zoo. 2021. Available online: https://content.govdelivery. com/accounts/USDAAPHIS/bulletins/2b5837f/ (accessed on 1 February 2022).

188. USDA; APHIS. Confirmation of COVID-19 in Otters at an Aquarium in Georgia Stakeholder Announcement. 2021. Available online: https://www.aphis.usda.gov/aphis/newsroom/stakeholder-info/SA_By_Date/SA-2021/SA-2004 (accessed on 1 February 2022).

189. Oreshkova, N.; Molenaar, R.J.; Vreman, S.; Harders, F.; Oude Munnink, B.B.; Hakze-van der Honing, R.W.; Gerhards, N.; Tolsma, P.; Bouwstra, R.; Sikkema, R.S.; et al. SARS-CoV-2 infection in farmed minks, The Netherlands, April and May 2020. *Eurosurveillance* **2020**, *25*, 2001005. [CrossRef]

190. Cai, H.Y.; Cai, A. SARS-CoV-2 spike protein gene variants with N501T and G142D mutation-dominated infections in mink in the United States. *J. Vet. Diagn. Investig.* **2021**, *33*, 939–942. [CrossRef] [PubMed]

191. Tan, C.C.S.; Datt Lam, S.; Richard1, D.; Owen, C.; Berchtold, D.; Orengo, C.; Surendran Nair, M.; Kuchipudi, S.V.; Kapur, V.; vanDorp, L.; et al. Transmission of SARS-CoV-2 from humans to animals and potential host adaptation. *bioRXiv* **2022**. [CrossRef]

192. Oude Munnink, B.B.; Sikkema, R.S.; Nieuwenhuijse, D.F.; Molenaar, R.J.; Munger, E.; Molenkamp, R.; van der Spek, A.; Tolsma, P.; Rietveld, A.; Brouwer, M.; et al. Transmission of SARS-CoV-2 on mink farms between humans and mink and back to humans. *Science* **2021**, *371*, 172–177. [CrossRef] [PubMed]

193. Mallapaty, S. COVID mink analysis shows mutations are not dangerous—Yet. *Nature* **2020**, *587*, 340–341. [CrossRef] [PubMed]

194. ProMED-Mail. COVID-19 Update (549): Animal, Mink, Denmark, Erad. Russia, Vaccine, China; RFI. ProMED 20201222.8039549. 2020. Available online: https://promedmail.org/promed-post/?id=8039549 (accessed on 28 January 2022).

195. Ahmed, R.; Hasan, R.; Siddiki, A.; Islam, M.S. Host range projection of SARS-CoV-2: South Asia perspective. *Infect. Genet. Evol.* **2021**, *87*, 104670. [CrossRef] [PubMed]

196. Bouricha, E.M.; Hakmi, M.; Akachar, J.; Belyamani, L.; Ibrahimi, A. In silico analysis of ACE2 orthologues to predict animal host range with high susceptibility to SARS-CoV-2. *3 Biotech* **2020**, *10*, 483. [CrossRef]

197. Damas, J.; Hughes, G.M.; Keough, K.C.; Painter, C.A.; Persky, N.S.; Corbo, M.; Hiller, M.; Koepfli, K.P.; Pfenning, A.R.; Zhao, H.; et al. Broad host range of SARS-CoV-2 predicted by comparative and structural analysis of ACE2 in vertebrates. *Proc. Natl. Acad. Sci. USA* **2020**, *117*, 22311–22322. [CrossRef]

198. Luan, J.; Lu, Y.; Jin, X.; Zhang, L. Spike protein recognition of mammalian ACE2 predicts the host range and an optimized ACE2 for SARS-CoV-2 infection. *Biochem. Biophys. Res. Commun.* **2020**, *526*, 165–169. [CrossRef]

199. Mykytyn, A.Z.; Lamers, M.M.; Okba, N.M.A.; Breugem, T.I.; Schipper, D.; van den Doel, P.B.; van Run, P.; van Amerongen, G.; de Waal, L.; Koopmans, M.P.G.; et al. Susceptibility of rabbits to SARS-CoV-2. *Emerg. Microbes Infect.* **2021**, *10*, 1–7. [CrossRef]

200. Palmer, M.V.; Martins, M.; Falkenberg, S.; Buckley, A.; Caserta, L.C.; Mitchell, P.K.; Cassmann, E.D.; Rollins, A.; Zylich, N.C.; Renshaw, R.W.; et al. Susceptibility of white-tailed deer (Odocoileus virginianus) to SARS-CoV-2. *J. Virol.* **2021**, *95*, e00083-21. [CrossRef]

201. Singh, D.K.; Singh, B.; Ganatra, S.R.; Gazi, M.; Cole, J.; Thippeshappa, R.; Alfson, K.J.; Clemmons, E.; Gonzalez, O.; Escobedo, R.; et al. Responses to acute infection with SARS-CoV-2 in the lungs of rhesus macaques, baboons and marmosets. *Nat. Microbiol.* **2021**, *6*, 73–86. [CrossRef] [PubMed]

202. Bertzbach, L.D.; Vladimirova, D.; Dietert, K.; Abdelgawad, A.; Gruber, A.D.; Osterrieder, N.; Trimpert, J. SARS-CoV-2 infection of Chinese hamsters (*Cricetulus griseus*) reproduces COVID-19 pneumonia in a well-established small animal model. *Transbound. Emerg. Dis.* **2021**, *68*, 1075–1079. [CrossRef] [PubMed]

203. Bosco-Lauth, A.M.; Hartwig, A.E.; Porter, S.M.; Gordy, P.W.; Nehring, M.; Byas, A.D.; VandeWoude, S.; Ragan, I.K.; Maison, R.M.; Bowen, R.A. Experimental infection of domestic dogs and cats with SARS-CoV-2: Pathogenesis, transmission, and response to reexposure in cats. *Proc. Natl. Acad. Sci. USA* **2020**, *117*, 26382–26388. [CrossRef] [PubMed]

204. Freuling, C.M.; Breithaupt, A.; Muller, T.; Sehl, J.; Balkema-Buschmann, A.; Rissmann, M.; Klein, A.; Wylezich, C.; Hoper, D.; Wernike, K.; et al. Susceptibility of Raccoon Dogs for Experimental SARS-CoV-2 Infection. *Emerg. Infect. Dis.* **2020**, *26*, 2982–2985. [CrossRef]

205. Imai, M.; Iwatsuki-Horimoto, K.; Hatta, M.; Loeber, S.; Halfmann, P.J.; Nakajima, N.; Watanabe, T.; Ujie, M.; Takahashi, K.; Ito, M.; et al. Syrian hamsters as a small animal model for SARS-CoV-2 infection and countermeasure development. *Proc. Natl. Acad. Sci. USA* **2020**, *117*, 16587–16595. [CrossRef]

206. Kim, Y.I.; Kim, S.G.; Kim, S.M.; Kim, E.H.; Park, S.J.; Yu, K.M.; Chang, J.H.; Kim, E.J.; Lee, S.; Casel, M.A.B.; et al. Infection and Rapid Transmission of SARS-CoV-2 in Ferrets. *Cell Host Microbe* **2020**, *27*, 704–709.e2. [CrossRef]

207. Lu, S.; Zhao, Y.; Yu, W.; Yang, Y.; Gao, J.; Wang, J.; Kuang, D.; Yang, M.; Yang, J.; Ma, C.; et al. Comparison of nonhuman primates identified the suitable model for COVID-19. *Signal Transduct. Target. Ther.* **2020**, *5*, 157. [CrossRef]

208. Munoz-Fontela, C.; Dowling, W.E.; Funnell, S.G.P.; Gsell, P.S.; Riveros-Balta, A.X.; Albrecht, R.A.; Andersen, H.; Baric, R.S.; Carroll, M.W.; Cavaleri, M.; et al. Animal models for COVID-19. *Nature* **2020**, *586*, 509–515. [CrossRef]

209. Shan, C.; Yao, Y.F.; Yang, X.L.; Zhou, Y.W.; Gao, G.; Peng, Y.; Yang, L.; Hu, X.; Xiong, J.; Jiang, R.D.; et al. Infection with novel coronavirus (SARS-CoV-2) causes pneumonia in Rhesus macaques. *Cell Res.* **2020**, *30*, 670–677. [CrossRef]

210. Sia, S.F.; Yan, L.M.; Chin, A.W.H.; Fung, K.; Choy, K.T.; Wong, A.Y.L.; Kaewpreedee, P.; Perera, R.; Poon, L.L.M.; Nicholls, J.M.; et al. Pathogenesis and transmission of SARS-CoV-2 in golden hamsters. *Nature* **2020**, *583*, 834–838. [CrossRef]

211. Trimpert, J.; Vladimirova, D.; Dietert, K.; Abdelgawad, A.; Kunec, D.; Dokel, S.; Voss, A.; Gruber, A.D.; Bertzbach, L.D.; Osterrieder, N. The Roborovski Dwarf Hamster Is A Highly Susceptible Model for a Rapid and Fatal Course of SARS-CoV-2 Infection. *Cell Rep.* **2020**, *33*, 108488. [CrossRef] [PubMed]

212. Ulrich, L.; Wernike, K.; Hoffmann, D.; Mettenleiter, T.C.; Beer, M. Experimental Infection of Cattle with SARS-CoV-2. *Emerg. Infect. Dis.* **2020**, *26*, 2979–2981. [CrossRef] [PubMed]

213. Schlottau, K.; Rissmann, M.; Graaf, A.; Schon, J.; Sehl, J.; Wylezich, C.; Hoper, D.; Mettenleiter, T.C.; Balkema-Buschmann, A.; Harder, T.; et al. SARS-CoV-2 in fruit bats, ferrets, pigs, and chickens: An experimental transmission study. *Lancet Microbe* **2020**, *1*, e218–e225. [CrossRef]

214. Suarez, D.L.; Pantin-Jackwood, M.J.; Swayne, D.E.; Lee, S.A.; DeBlois, S.M.; Spackman, E. Lack of Susceptibility to SARS-CoV-2 and MERS-CoV in Poultry. *Emerg. Infect. Dis.* **2020**, *26*, 3074–3076. [CrossRef]

215. Wang, M.; Cao, R.; Zhang, L.; Yang, X.; Liu, J.; Xu, M.; Shi, Z.; Hu, Z.; Zhong, W.; Xiao, G. Remdesivir and chloroquine effectively inhibit the recently emerged novel coronavirus (2019-nCoV) in vitro. *Cell Res.* **2020**, *30*, 269–271. [CrossRef] [PubMed]

216. Liu, J.; Cao, R.; Xu, M.; Wang, X.; Zhang, H.; Hu, H.; Li, Y.; Hu, Z.; Zhong, W.; Wang, M. Hydroxychloroquine, a less toxic derivative of chloroquine, is effective in inhibiting SARS-CoV-2 infection in vitro. *Cell Discov.* **2020**, *6*, 16. [CrossRef]

217. Dittmar, M.; Lee, J.S.; Whig, K.; Segrist, E.; Li, M.; Kamalia, B.; Castellana, L.; Ayyanathan, K.; Cardenas-Diaz, F.L.; Morrisey, E.E.; et al. Drug repurposing screens reveal cell-type-specific entry pathways and FDA-approved drugs active against SARS-Cov-2. *Cell Rep.* **2021**, *35*, 108959. [CrossRef]

218. Ko, M.; Jeon, S.; Ryu, W.S.; Kim, S. Comparative analysis of antiviral efficacy of FDA-approved drugs against SARS-CoV-2 in human lung cells. *J. Med. Virol.* **2021**, *93*, 1403–1408. [CrossRef]

219. Boulware, D.R.; Pullen, M.F.; Bangdiwala, A.S.; Pastick, K.A.; Lofgren, S.M.; Okafor, E.C.; Skipper, C.P.; Nascene, A.A.; Nicol, M.R.; Abassi, M.; et al. A Randomized Trial of Hydroxychloroquine as Postexposure Prophylaxis for Covid-19. *N. Engl. J. Med.* **2020**, *383*, 517–525. [CrossRef]

220. Weston, S.; Coleman, C.M.; Haupt, R.; Logue, J.; Matthews, K.; Li, Y.; Reyes, H.M.; Weiss, S.R.; Frieman, M.B. Broad Anti-coronavirus Activity of Food and Drug Administration-Approved Drugs against SARS-CoV-2 In Vitro and SARS-CoV In Vivo. *J. Virol.* **2020**, *94*, e01218-20. [CrossRef]

221. Kaptein, S.J.F.; Jacobs, S.; Langendries, L.; Seldeslachts, L.; Ter Horst, S.; Liesenborghs, L.; Hens, B.; Vergote, V.; Heylen, E.; Barthelemy, K.; et al. Favipiravir at high doses has potent antiviral activity in SARS-CoV-2-infected hamsters, whereas hydroxychloroquine lacks activity. *Proc. Natl. Acad. Sci. USA* **2020**, *117*, 26955–26965. [CrossRef] [PubMed]

222. Rosenke, K.; Jarvis, M.A.; Feldmann, F.; Schwarz, B.; Okumura, A.; Lovaglio, J.; Saturday, G.; Hanley, P.W.; Meade-White, K.; Williamson, B.N.; et al. Hydroxychloroquine Proves Ineffective in Hamsters and Macaques Infected with SARS-CoV-2. *bioRxiv* **2020**. [CrossRef]

223. Hoffmann, M.; Kleine-Weber, H.; Pohlmann, S. A Multibasic Cleavage Site in the Spike Protein of SARS-CoV-2 Is Essential for Infection of Human Lung Cells. *Mol. Cell* **2020**, *78*, 779–784. [CrossRef]

224. Pohl, M.O.; Busnadiego, I.; Kufner, V.; Glas, I.; Karakus, U.; Schmutz, S.; Zaheri, M.; Abela, I.; Trkola, A.; Huber, M.; et al. SARS-CoV-2 variants reveal features critical for replication in primary human cells. *PLoS Biol.* **2021**, *19*, e3001006. [CrossRef]

225. Peacock, T.P.; Goldhill, D.H.; Zhou, J.; Baillon, L.; Frise, R.; Swann, O.C.; Kugathasan, R.; Penn, R.; Brown, J.C.; Sanchez-David, R.Y.; et al. The furin cleavage site in the SARS-CoV-2 spike protein is required for transmission in ferrets. *Nat. Microbiol.* **2021**, *6*, 899–909. [CrossRef] [PubMed]

226. Liu, Z.; Zheng, H.; Lin, H.; Li, M.; Yuan, R.; Peng, J.; Xiong, Q.; Sun, J.; Li, B.; Wu, J.; et al. Identification of Common Deletions in the Spike Protein of Severe Acute Respiratory Syndrome Coronavirus 2. *J. Virol.* **2020**, *94*, e00790-20. [CrossRef]

227. Saito, A.; Irie, T.; Suzuki, R.; Maemura, T.; Nasser, H.; Uriu, K.; Kosugi, Y.; Shirakawa, K.; Sadamasu, K.; Kimura, I.; et al. Enhanced fusogenicity and pathogenicity of SARS-CoV-2 Delta P681R mutation. *Nature* **2021**, *602*, 300–306. [CrossRef]

228. Mlcochova, P.; Kemp, S.A.; Dhar, M.S.; Papa, G.; Meng, B.; Ferreira, I.; Datir, R.; Collier, D.A.; Albecka, A.; Singh, S.; et al. SARS-CoV-2 B.1.617.2 Delta variant replication and immune evasion. *Nature* **2021**, *599*, 114–119. [CrossRef]

229. Caly, L.; Druce, J.; Roberts, J.; Bond, K.; Tran, T.; Kostecki, R.; Yoga, Y.; Naughton, W.; Taiaroa, G.; Seemann, T.; et al. Isolation and rapid sharing of the 2019 novel coronavirus (SARS-CoV-2) from the first patient diagnosed with COVID-19 in Australia. *Med. J. Aust.* **2020**, *212*, 459–462. [CrossRef]

230. Singh, J.; Rahman, S.A.; Ehtesham, N.Z.; Hira, S.; Hasnain, S.E. SARS-CoV-2 variants of concern are emerging in India. *Nat. Med.* **2021**, *27*, 1131–1133. [CrossRef]

231. Peacock, T.P.; Brown, J.C.; Zhou, J.; Thakur, N.; Newman, J.; Kugathasan, R.; Sukhova, K.; Kaforou, M.; Bailey, D.; Barclay, W.S. The SARS-CoV-2 variant, Omicron, shows rapid replication in human primary nasal epithelial cultures and efficiently uses the endosomal route of entry. *bioRxiv* **2022**. [CrossRef]

232. Halfmann, P.J.; Iida, S.; Iwatsuki-Horimoto, K.; Maemura, T.; Kiso, M.; Scheaffer, S.M.; Darling, T.L.; Joshi, A.; Loeber, S.; Singh, G.; et al. SARS-CoV-2 Omicron virus causes attenuated disease in mice and hamsters. *Nature* **2022**. [CrossRef] [PubMed]

233. Abdelnabi, R.; Foo, C.S.; Zhang, X.; Lemmens, V.; Maes, P.; Slechten, B.; Raymenants, J.; Andre, E.; Weynand, B.; Dallmeier, K.; et al. The omicron (B.1.1.529) SARS-CoV-2 variant of concern does not readily infect Syrian hamsters. *Antiviral Res.* **2022**, *198*, 105253. [CrossRef] [PubMed]

234. Abdullah, F.; Myers, J.; Basu, D.; Tintinger, G.; Ueckermann, V.; Mathebula, M.; Ramlall, R.; Spoor, S.; de Villiers, T.; Van der Walt, Z.; et al. Decreased severity of disease during the first global omicron variant COVID-19 outbreak in a large hospital in tshwane, South Africa. *Int. J. Infect. Dis.* **2021**, *116*, 38–42. [CrossRef] [PubMed]

235. McCallum, M.; Czudnochowski, N.; Rosen, L.E.; Zepeda, S.K.; Bowen, J.E.; Walls, A.C.; Hauser, K.; Joshi, A.; Stewart, C.; Dillen, J.R.; et al. Structural basis of SARS-CoV-2 Omicron immune evasion and receptor engagement. *Science* **2022**, *375*, 864–868. [CrossRef]